THE DESIGN, CONSTRUCTION, OUTFITTING, AND PRELIMINARY TESTING OF THE C-SCOUT AUTONOMOUS UNDERWATER VEHICLE (AUV)

TIMOTHY CURTIS

The Design, Construction, Outfitting, and Preliminary Testing of the C-SCOUT Autonomous Underwater Vehicle (AUV)

By
©Timothy Curtis, B. Eng.

A Thesis Submitted to the School of Graduate Studies in Partial Fulfillment for the Degree of Master of Engineering

Faculty of Engineering and Applied Science
Memorial University of Newfoundland

October, 2001

St. John's, Newfoundland, Canada

ABSTRACT

This thesis presents and discusses the design process, construction, outfitting, and preliminary in-water testing of the C-SCOUT (Canadian Self-Contained Off-the-shelf Underwater Testbed) Autonomous Underwater Vehicle (AUV). This work was carried out from January 1999 to August 2001. C-SCOUT was designed to be of low cost and simple to manufacture while still retaining a multi-mission capability. The designed vehicle is for graduate student research with a limited budget, and is designed to be easily modifiable, small enough to be easily handled, highly maneuverable, and readily adaptable for many missions. A modular design was developed, and the most basic version of the AUV was built and tested as a proof-of-concept vehicle.

The C-SCOUT Baseline Configuration vehicle is 2.7 metres long, 0.4 metres in diameter, and 1.06 metres from fin-tip to fin-tip. A second vehicle hull, the C-SCOUT II, has been constructed for hydrodynamic testing on the planar motion mechanism. The control surfaces were designed using Det Norkse Veritas guidelines for highly maneuverable vessels and an in-depth analysis of pressure vessel design was carried out using boiler code from the American Society of Mechanical Engineers. Vehicle powering requirements were estimated using a component buildup method and an empirical data-base method. Both yielded very similar results. Preliminary in-water tests were conducted to validate the vehicle design methodology. The C-SCOUT AUV performed well in these trials and can now be used as a testbed vehicle for graduate level research.

ACKNOWLEDGEMENTS

My sincerest appreciation goes out to Dr. Chris Williams and Dr. Neil Bose for their support, guidance, and research support funding throughout this thesis. Their acceptance of trying new techniques made C-SCOUT come together in short order.

Financial support came from Memorial University of Newfoundland (MUN), the Institute for Marine Dynamics (IMD) of the National Research Council of Canada (NRCC), and an NSERC (Natural Sciences and Engineering Research Council of Canada) Strategic Project entitled "*Ocean Environmental Risk Engineering Using Autonomous Underwater Vehicles.*"

I would also like to thank the other past and present members of Team C-SCOUT for the contributions they provided to the project: Renee Boileau, Lucas Gray, Erin MacNeil, Doug Perrault, Doug Pittman, Sheila Pomroy, Lloyd Smith, Steve Taylor, Meggan Vickerd, and Dan Vyselaar. Other sources of technical support who I would like to thank are Trent Slade, Jim Everhard, Mike Walsh, Enos Harnum, John Hagerty, Spence Butt, Andy Wallace, John Bell, the IMD electronics shop crew, MUN Technical Services, and everyone else at IMD for moral support. Additionally, I would like to thank those who kept my sanity over the past two years and who periodically provided chocolate nourishment – Arlene Sare and Millie Chafe. Finally, I would like to thank my family and friends for listening to C-SCOUT stories and Newfoundland weather horror stories while providing long-distance encouragement.

The C-SCOUT project is part of a collaborative venture partially funded by a five year NSERC Strategic Grant entitled, "*Ocean Environmental Risk Engineering Using Autonomous Underwater Vehicles*". This grant, aimed at environmental effects monitoring and assessment of offshore petroleum discharges, involves the following research and industrial partners:

Research Partners:

Ocean Engineering Research Centre (OERC) and

Instrumentation, Control and Automation (INCA) Centre

Memorial University of Newfoundland (MUN)

- OERC objectives are to form a focus for ocean related engineering research from all disciplines in the Faculty of Engineering and Applied Science and to build cross disciplinary links to other parts of the University, institutions and industry. Ocean engineering research at MUN is very strong with one of its main strengths being the diversity of projects and researchers that have been and are associated with the Centre.

- INCA is an industrial outreach centre of excellence with expertise in the computerized embedded systems. INCA is part of MUN whose response is to the development of the oil and gas industry off the coast of Newfoundland and Labrador. This is an education and research centre adjacent to the oil patch and committed to excellence in instrumentation, control and automation.

Institute for Marine Dynamics (IMD)

National Research Council of Canada (NRCC)

- IMD was established in St. John's, Newfoundland, in 1985 as Canada's national centre for ocean technology research and development. It provides innovative solutions and technical expertise in support of Canadian industry, and collaborates with international companies and research agencies to bring new technology to Canada. The Institute's capability is unique to the nation and no other organization offers the combination of knowledge, experience and world-class facilities.

C-CORE

- Since 1975, C-CORE in St. John's, NF activities have grown to include applied research and development, technology transfer and technology demonstration, commercialization of intellectual property and specialized advisory services to a wide range of industries.

Space and Subsea Robotics Laboratory

University of Victoria

- The subsea activities of the Space and Subsea Robotics Laboratory encompass both autonomous and remotely-operated undersea vehicles (AUVs and ROVs), as well as towed and tethered marine systems, including moored buoys.

Industrial Partners:

Petro-Canada through the Terra Nova Alliance

- A major Canadian oil and gas company who are currently operators of the Terra Nova oil field in the Jeanne d'Arc Basin with a strong reputation for environmental stewardship and corporate responsibility.

International Submarine Engineering Ltd. (ISE)

- International Submarine Engineering Ltd. is a world player in the design and development of autonomous and remotely operated underwater vehicles (AUVs and ROVs) and robotic systems.

Geo-Resources Inc. (GRI)

- Geo-Resources Inc. is a privately owned Canadian company, which was established in 1986 whose mandate at that time was to provide ocean mapping services for domestic and international customers. In recent years the focus has shifted toward research and development projects with an emphasis on creating commercially viable software based products. GRI has experience in areas such as multibeam sonar mapping, tidal monitoring, GPS positioning, and operation of remotely controlled vehicles for anti-submarine warfare and mine hunting trials.

Team Members:

Graduate Students:

Timothy Curtis - Responsible for the design, construction, outfitting, and preliminary testing of the C-SCOUT AUV.

Mukhtasor – Studied dispersion modeling of undersea plumes discharged from offshore drilling platforms.

Vanessa Pennell – Studied environmental monitoring using autonomous underwater vehicles.

Doug Perrault – Dynamics and control of underwater vehicle behaviors.

Doug Pittman – Studied sonar returns and mapping.

Rehan Sadiq – Studied fates modeling of undersea plumes.

Aaron Saunders – Developing a through-body thruster system for the C-SCOUT AUV.

Lloyd Smith – Completed initial wiring and coding for C-SCOUT; assisted electrical students on a part-time basis.

Steve Taylor - Developing an autonomous controller for an AUV based on a Distributed Microcontroller Architecture.

Roy Thomas – Responsible for completing the second phase of in-water experiments with the C-SCOUT AUV.

Work Term Students:

Hermen Bijleveld - Responsible for developing, constructing, and testing a highly efficient propulsion system for the C-SCOUT AUV.

Renee Boileau – Worked on the initial design spiral for the C-SCOUT AUV.

Timothy Curtis – Worked on the initial design spiral for the C-SCOUT AUV.

Lucas Gray – Machined the majority of the C-SCOUT AUV structural components.

Erin MacNeil - Machine work on C-SCOUT and testing of the control surfaces.

Sheila Pomroy – Assisted in the rebuilding of the C-SCOUT computer system.

Steve Taylor - Responsible for rebuilding and ruggedizing the C-SCOUT onboard electronics and software, and some systems integration.

Meggan Vickerd - Responsible for machining and constructing some parts of C-SCOUT and also machined C-SCOUT II.

Dan Vyselaar – Assisted in developing a mounting system to attach C-SCOUT II to the planar motion mechanism for hydrodynamic testing.

TABLE OF CONTENTS

Abstract.....i

Acknowledgements.....ii

Table of Contents.....ix

List of Figures.....xii

List of Acronyms.....xv

Chapter 1 – Introduction and History

1.1 Introduction.....1

1.2 Background and History.....2

Chapter 2 – Overall Vehicle Design

2.1 Objective.....9

2.2 Vehicle Purpose and Applications.....10

2.3 Vehicle Design.....11

2.4 Hull Design.....14

Chapter 3 – Detailed Design

3.1 The C-SCOUT AUV.....18

3.2 Modularity.....18

3.3 Range of Hull Configurations.....19

3.4 Overall Vehicle Particulars.....22

3.5 C-SCOUT General Arrangement.....22

3.6 Hull Fabrication.....23

3.7 Powering Options.....27

Chapter 4 – Design Calculations

4.1 Propulsor....35

4.2 Control Surface Design....40

4.3 Pressure Vessel Design....45

Chapter 5 – Onboard Systems

5.1 Internal Components....66

5.2 Computer System....67

5.3 Flotation....71

5.4 Control System....73

5.5 Navigation System Planned for Future Testing....73

5.6 Proposed Emergency Systems....76

Chapter 6 – Vehicle Deployment

6.1 C-SCOUT Carriage....78

6.2 C-SCOUT Launch Procedure....79

Chapter 7 – Vehicle Testing

7.1 C-SCOUT Preliminary Testing....82

Chapter 8 – Conclusions and Recommendations

8.1 Conclusions....86

8.2 Recommendations....88

References....89

Bibliography....93

Appendix A – Powering Calculations

Appendix B – Control Surface Sizing

Appendix C – Pressure Vessel Design

Appendix D – Testing Phase Two

LIST OF FIGURES

1.2.1 American AUV XP-21.....7

1.2.2 British AUV AutoSub.....7

2.3.1 Japanese AUV Twin Burger.....11

2.3.2 Norwegian AUV Hugin.....12

2.4.1 Plot of drag coefficient vs. diameter/length ratio for streamlined bodies.....15

2.4.2 AUV design spiral.....17

3.3.1 C-SCOUT AUV Baseline Configuration.....20

3.3.2 C-SCOUT AUV Fully-Actuated Configuration.....21

3.5.1 General arrangement of the C-SCOUT AUV.....23

3.6.1 C-SCOUT nose and tail module production.....24

3.6.2 C-SCOUT module flange.....25

3.6.3 C-SCOUT modular framework design.....25

3.6.4 Endplate flange being machined.....26

3.7.1 AUV R-One – closed-cycle Diesel engine powered.....28

3.7.2 Solar AUV – solar powered.....29

3.7.3 SLOCUM AUV – ocean thermal energy powered.....30

3.7.4 Table of battery power densities.....31

3.7.5 Battery vents sealed with Renshape™ box.....33

4.1.1 C-SCOUT drag predictions.....36

4.1.2 Tecnadyne 1020 Thruster.....37

4.1.3 Drag & thrust estimates for C-SCOUT Baseline Configuration.....38

4.1.3 Minnkota 35T trolling motor mounted in tail.....40

4.2.1 Control surface major dimensions.....41

4.2.2 Control surface geometry and attachment scheme.....42

4.2.3 Mold for control surfaces.....43

4.2.4 Actuator motor and housing.....44

4.3.1 Chart of pressure vessels with simple ring stiffeners.....50

4.3.2 Chart of pressure vessels with small T-bar ring stiffeners.....51

4.3.3 Chart of pressure vessels with large T-bar ring stiffeners.....53

4.3.4 Chart of pressure vessels with triangular ring stiffeners.....54

4.3.5 Comparison chart of ring-stiffened pressure vessels.....55

4.3.6 Pressure vessel optimization curve for C-SCOUT pressure vessel.....57

4.3.7 Correlation between cross-sectional area and achievable depth.....59

4.3.8 Effect of stiffener arrangement on pressure vessel design.....61

4.3.9 Comparison of optimization equation and calculations for geometry changes....63

4.3.10 Comparison of optimization equation and calculations for material changes.....64

5.1.1 Chassis for electronics components.....66

5.2.1 Sonar mounting location.....68

5.2.2 Cable tunnels through battery module.....70

5.3.1 Drainage and venting holes in skin.....72

5.5.1 Canadian AUV Dolphin.....74

6.1.1 C-SCOUT Carriage.....78

6.2.1 Pressure vessel brackets.....79

6.2.2 Battery stack and placement.....80

6.2.3 Stringer adjustment screws.....81

7.1.1 C-SCOUT operating with umbilical.....83

7.1.2 C-SCOUT operating entirely submerged.....85

LIST OF ACRONYMS

AUV – Autonomous Underwater Vehicle – An unmanned underwater vehicle controlled by an onboard computer with sensory input and an onboard power supply.

BC – Baseline Configuration – A possible configuration of C-SCOUT.

C-SCOUT – Canadian Self-Contained Off-the-shelf Underwater Testbed

DGPS – Differential Global Positioning System

EMF – Electro-Magnetic Field

FAC – Fully-Actuated Configuration – A possible configuration of C-SCOUT.

GRI – Geo-Resources, Inc.

IMD – Institute for Marine Dynamics

INCA – Instrumentation, Control, and Automation Lab, MUN

ISE – International Submarine Engineering

MOSFET - Metal-Oxide Semiconductor Field-Effect Transistor

MUN – Memorial University of Newfoundland

NRC – National Research Council

NRCC – National Research Council of Canada

NSERC - Natural Sciences and Engineering Research Council of Canada

OERC – Ocean Engineering Research Centre

ROV – Remotely Operated Vehicle – An unmanned underwater vehicle tethered to a mother ship and operated through an umbilical by a human operator.

SCUBA – Self-Contained Underwater Breathing Apparatus

VIP – Versatile Instrumentation Platform – A possible configuration of C-SCOUT.

Chapter 1 – Introduction and History

1.1 INTRODUCTION

An Autonomous Underwater Vehicle (AUV) is a self-propelled submersible robot capable of carrying out pre-programmed tasks without human intervention. An AUV can be hundreds of miles from any support vessel or shoreline, and completely out of contact with any external input for hours or days at a time while it completes its mission. AUVs are particularly suited for hazardous applications because they do not require a human support team nearby or a tether to the surface. Therefore, they can, for example, find and classify undersea mines or examine the underneath of ice sheets without risking human injury or life.

As an ocean-going nation, Canada needs to have full grasp of the tools for ocean exploration and resource development. AUVs are emerging as a commercially viable technology as ocean exploration heads into deeper waters. Without the encumbrance of a tether or the need for a support ship, these vehicles provide a platform for a wide variety of offshore tasks, including:

- Environmental Monitoring
- Offshore Oil and Gas Systems Maintenance and Support
- Iceberg Profiling and Tracking and Under-Ice Mapping
- Pipeline Surveys

- Telecommunications Cable Surveys
- Mine Detection and Countermeasures
- Oceanographic Sampling and Research
- Hydrographic Surveys

The C-SCOUT AUV was designed to serve as a testbed for graduate level research focusing on control systems and vehicle endurance.

1.2 BACKGROUND AND HISTORY

The desire to study and work beneath the ocean's waves dates back to the beginning of recorded history. The first diving bells were conceived in the 1600s by Halley and Kessler (McFarlane, 1993), and since then, the development goals have been to extend the depth, duration, and capabilities of underwater work systems. By the end of the 1960s, there were numerous manned submersibles, the self-contained underwater breathing apparatus (SCUBA) had been developed, and the very first remotely operated vehicles (ROVs) were making headlines. The costs and limitations of humans in the sea gave the ROV a definite advantage. According to McFarlane, "To put a diver on the bottom in 220 meters of water would require 50 tons of equipment and a team of 25 people, including a doctor. On completion of the dive, decompression would take 7 days. A crew would be required 24 hours a day to monitor the diver. If 85 percent of the helium used is reclaimed, the cost of the 15 percent of lost helium exceeds $10,000 per

day." It is clear that this method for underwater work is unrealistic for prolonged commercial use.

The ROV came into widespread commercial usage in the late 1970s, and today there are numerous companies specializing in their construction and modification. Many offshore oil and gas companies use ROVs for inspecting pipelines, flanges, connections, and even offshore platforms. Since the duration of the ROV's mission is limited only by the operator's endurance, and there are no concerns about decompression or loss of life, the ROV is a more than viable tool.

However, the limitations of ROVs appear in more complex missions. These include pipeline inspections, deepwater operation, inspections where cables may become snagged such as inside shipwrecks or around pilings and legs of offshore platforms, mine inspection and countermeasures, high-speed operations, long-range operations, and multiple vehicle operations. Another major problem inherent with ROVs is deep-water snap loading of the umbilical induced by wave motion which can cause the cable to sever. All of these limitations stem from the fact that an ROV is literally tied to a mother ship by a cable that imposes severe restrictions on vehicle mobility and agility. As the use of ROVs becomes more widespread, and their tasking more complex in deeper waters, there is a need to free the vehicle from the power and signal tether, and to increase both the level of control autonomy and the maneuvering precision (Healey, *et al.*, 1994).

An AUV (Autonomous Underwater Vehicle) is a self-powered, self-propelled underwater vehicle capable of performing a predetermined mission without the need of a crew for monitoring or control. Therefore, an AUV could be hundreds of miles from any support vessel or shoreline, and completely out of contact with any external source for hours or days at a time (limited only by power supply) while it performs its mission.

An ROV must have proportionally larger motors than an AUV because in order to maintain mobility, it must have the power to drag its cable. For example, a vehicle that requires 2.5 hp to propel itself at three knots would require 40 hp to propel itself if it had a 1,000-foot long cable attached (McFarlane, 1993). Thus for a 1,000 foot range of mobility, without moving the location of the winch, the ROV needs 15 times more power than a comparable AUV, and that factor increases drastically with increased range. Deepwater ROVs, therefore, are very heavy, some weighing as much as 8,500 kg (McFarlane, 1993). This size of vehicle requires a hefty support vessel with a large overboard crane and the necessary crew to operate it. An AUV designed for the same depth could be a small fraction of the weight. That weight could easily be picked up by a few people, and minimal special handling equipment would be required.

Another advantage of the AUV is that it can be deployed far away from its intended search site while an ROV must be deployed directly over the search location. AUVs are particularly suited for hazardous applications because they do not require a human

support team nearby or a tether to the surface. This distance from a base is particularly helpful for ships engaging in minehunting, where the AUV could be 100 miles or more away from the support vessel. Mines are a major threat to ships and can completely destroy a naval force. During the Korean War, Admiral Harold Smith said about mines, "The US Navy has lost control of the sea to a country without a navy, employing a weapon obsolete at the time of the First World War, laid from vessels that were in use at the time of the birth of Christ" (McFarlane, 1993). A fleet of autonomous underwater vehicles could quickly and efficiently sweep a mine field and clear a safe path for vessels to transit. This type of usage for an AUV completely eliminates the human factor, so that if anything goes wrong, all that are lost are some electronics and motors which, although expensive, are much easier to replace than human lives.

The overhead costs associated with operating a large research vessel with a tethered data collection system impose a strict minimum on the data collected at any given time due to the number of simultaneously deployable instrumentation platforms. Because of the overhead, significant improvements in sampling technology on the tethered platform can produce only modest gains in the cost effectiveness. An AUV, or a research vessel deploying multiple AUVs, would increase the cost effectiveness of the data collection significantly by quickly and cheaply increasing the number of distinct observation platforms (Smith, *et al.*, 1995). AUVs used in oceanographic sampling also have much less of a physical impact on the environment and the very water being sampled when compared to that of a ship.

Since autonomous underwater vehicles are fairly new developments, most people are skeptical about their abilities and reliability. Before an AUV is launched into the sea, it must undergo rigorous trials in a test pool or a shallow lake until its control system can be fully trusted in autonomous operation. These trials can take years, and by the time the vehicle is fully developed, technology will have advanced far beyond where it was at the beginning of development. Components cannot be swapped for fear of a change in vehicle performance. For example, the Ocean Explorer AUV, when it was built about five years ago, could not use any off-the-shelf controllers because they were unable to fit within the hull diameter of 21 inches (Smith, *et al.*, 1994). Today, these controllers are about the size of a credit card, and they will continue to become smaller as time progresses. As a result of this technological development, almost all of the AUVs currently in existence are quite large, and still require a major surface effort to keep the vehicle in operation. (See Figures 1.2.1 and 1.2.2) This requirement for substantial surface support almost defeats the purpose of an AUV.

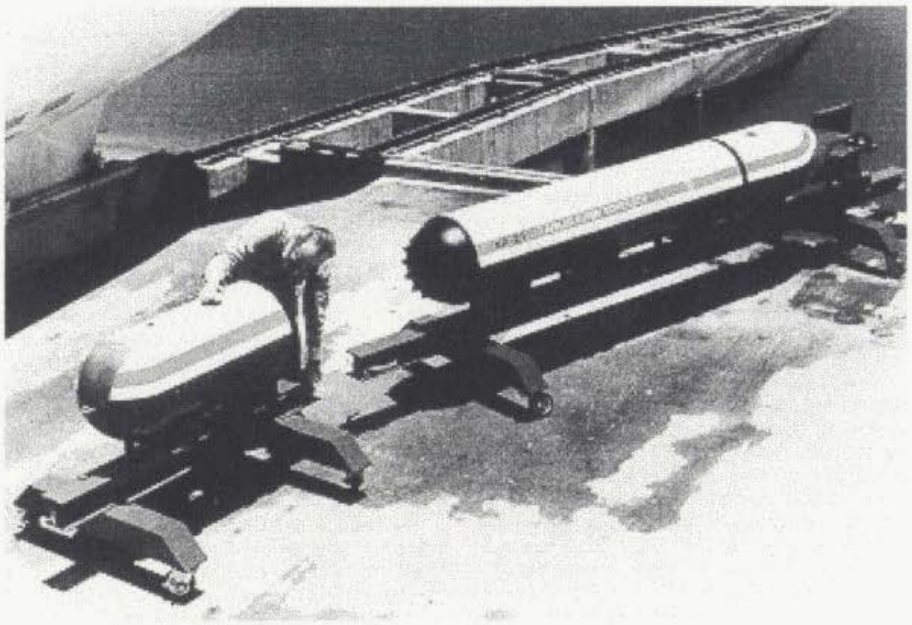

Figure 1.2.1: The AUV XP-21 by Applied Remote Technology Inc., USA. Note the large vehicle size (8.5 meter length). (Funnell, 1998)

Figure 1.2.2: The AUV AutoSub. Again note the large vehicle and complex handling system required. Courtesy of Southampton Oceanography Centre, UK.

In September of 1998, a collaborative effort between the Institute for Marine Dynamics (IMD) of the National Research Council of Canada and the Ocean Engineering Research Centre (OERC) of Memorial University of Newfoundland began to design a streamlined AUV to serve as a testbed for IMD and graduate level research. This AUV, the C-SCOUT, is expected to serve as a test-bed to assist in the development of future control and propulsion systems, the testing of vehicle components, and as a general research and development tool for years to come. Future versions of C-SCOUT can be configured for a wide variety of missions including search and survey, under ice operations, iceberg profiling, oceanographic sampling, and mine detection and countermeasures.

Chapter 2 – Overall Vehicle Design

2.1 OBJECTIVE

This thesis develops the design, construction and outfitting details, and the preliminary operational performance of a small, low-cost autonomous underwater vehicle that can be used with minimal surface/shore support to allow for completely autonomous operation for a wide variety of missions. A vehicle that uses off-the-shelf components benefits from the cost savings of a larger market, and any standard protocols used allow inter-operability between sensor and control systems from different manufacturers (Smith, *et al.*, 1995). The minimum operating conditions that were chosen to make this vehicle the most multifunctional design possible for testbed research are discussed herein.

First, the vehicle is desired to be high speed, as AUVs go. The desired forward speed is eight knots, with a reverse speed of four knots, and the vehicle should have a high degree of high speed and low speed maneuverability including hover capability. The AUV must be able to operate in a depth of 10 metres which corresponds to the deepest test tank depth available to us for testing. To eliminate the need for surface vessel support, and the associated costs, the vehicle should be as small as possible, and as lightweight as possible. These size and weight requirements would make the vehicle easy to deploy, easy to retrieve, and easy to transport. Since the designed AUV is to serve as a testbed for graduate level research, it should be readily modifiable and easy to construct. Lastly,

the vehicle should be as inexpensive as possible, without sacrificing reliability or functionality.

The development and construction of this vehicle is designed to be completed in stages. The simplest complete design is developed in this thesis for proof-of-concept testing, while leaving many open doors for future work. The main goal of this work was to develop an operational vehicle that can be adapted and modified to fulfill the ultimate aims of the project. The developed vehicle is not yet autonomous however.

2.2 VEHICLE PURPOSE AND APPLICATIONS

The developed AUV is designed to serve as a testbed to assist in the development of future control, power and propulsion systems, the testing of vehicle components, testing of onboard sensor packages for particular missions such as water sampling, and as a general research and development tool for years to come. Future versions of the AUV can be configured for a wide variety of missions including search and survey, under ice operations, iceberg profiling, oceanographic sampling, mine detection and countermeasures, and environmental monitoring. One particular application the vehicle is intended to be used for in the near future is monitoring around offshore oil rigs, specifically looking at offshore discharges of produced water, rock cuttings, and drilling mud. Many sensors are readily available to measure the necessary chemicals or

compositions in the water so the vehicle would in effect become a utility tool for transporting the equipment to and from a measuring station.

2.3 VEHICLE DESIGN

The design of an Autonomous Underwater Vehicle is driven by the intended mission. Vehicles that are designed to study and monitor a very small patch of the ocean floor, such as a single geothermal vent, are designed without consideration for hydrodynamic effects, since any motion is of short distance and low velocity. These vehicles, such as the Twin Burger 2 shown below (Figure 2.3.1), generally look like typical caged ROVs.

Figure 2.3.1: The AUV Twin Burger 2 by URA Laboratory, Institute of Industrial Science, University of Tokyo, Japan. Note the hydrodynamically inefficient form common to short-range AUVs.

AUVs that are designed to spend most of their time cruising are made to be as hydrodynamically efficient as possible, since a major limiting factor in vehicle endurance is the onboard power supply. An efficient form allows for a much greater cruising range for the same power supply, or a smaller, lighter vehicle with an equal cruising range. A good hydrodynamic design will yield two to ten times the range of a poor one at the same speed and depth by reducing the drag (Paster, 1986). A well-designed shape can also drastically reduce noise and instability, even at low speeds (Paster, 1986). Of course, there is a design balance between efficiency and ease of construction. A vehicle designed completely for efficiency is comprised entirely of complex curvature. It is therefore extremely difficult and expensive to manufacture out of metals, and even composites may not have the required strength or uniformity for a deepwater application. Nevertheless, some companies do build successful vehicles this way, for example the AUV Hugin by Kongsberg Simrad AS, Norway, and the Norwegian Defence Research Establishment (see Figure 2.3.2).

Figure 2.3.2: The Norwegian AUV, Hugin (Courtesy of Kongsberg-Simrad)

The Hugin is a viable commercial AUV that has been used in a number of survey situations and found to provide significant cost savings over conventional shipboard surveys. The Hugin is noted for its low noise level while underway, making it a prime operational platform for acoustic sensors.

The main design principle for achieving cost effectiveness and multi-utility is modularity, which needs to be systematic and must include every onboard system (Smith, *et al.*, 1994). Most streamlined AUVs are designed to have an axi-symmetric shape (circular cross-section) with an efficient nose and afterbody, and a large section of constant diameter midbody. This design allows for simplicity of construction and handling of the vehicle. Another advantage of having a vehicle with a parallel midbody is modularity of components. Modules of varied length can be inserted into the parallel midbody with little effect on the hydrodynamics. The hull is also much easier to manufacture since the parallel midbody modules are simple cylindrical sections that can be manufactured at any machine shop with a milling machine. The nose and tail of the vehicle are of utmost importance from the standpoint of hydrodynamic and propulsive efficiency. Since the same nose and tail can be used for any length parallel midbody, a complex shape can be economically justified. These constraints led to an ellipsoidal nose and a cubic spline tail for optimal flow characteristics and low drag as the choice for the present design.

Every step was taken to reduce any protuberances on the hull and to make the vehicle axisymmetric. Even a small uneven disruption on the hull can have drastic effects. For example, the battery sea-water scoop on a mid-1950s torpedo, shaped like a cylinder, caused roll and yaw instability due to vortex shedding, and increased the overall vehicle drag by 35%. A redesign of this intake by simple fairing eliminated the roll and yaw instabilities, and increased the original overall vehicle drag by only 6%, which is considerably less than the initial 35% increase (Paster, 1986). Extra emphasis on hull design will dramatically increase mission time in the long run.

2.4 HULL DESIGN

The length-to-diameter ratio (L/D) should be about seven or eight for optimum balance between hydrodynamic and volumetric efficiency. Vehicles with the same volume, but with an L/D lower than seven (D/L ratio of greater than 0.14) have marked increases in drag (See Figure 2.4.1), while vehicles over this ratio become too long and slender to maneuver well and have an inefficient interior volume. Differing lengths of parallel midbody, depending on the mission, will change this ratio, but on the average it will have a high efficiency if kept between an L/D of 6.5 and 9 (D/L of approximately 0.15 to 0.11).

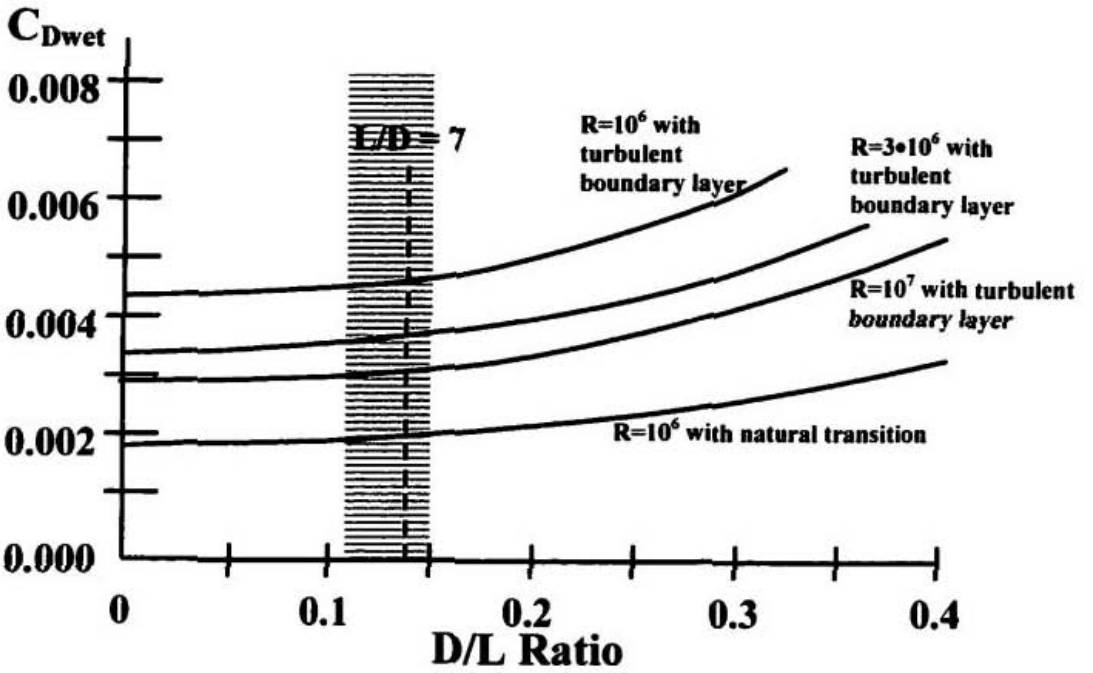

Figure 2.4.1: Variation of drag coefficient (based on wetted surface area) as a function of diameter-to-length ratio for a series of streamlined bodies for various Reynolds Numbers and boundary layers. The shaded bar is the optimal design region for this vehicle. Adapted from Hoerner, 1965.

The actual dimensions of the vehicle depend on the maximum size of the internal components. With the available technologies today, very small microprocessor-controlled components can be installed, and therefore the overall vehicle size can be considerably smaller than one built five years ago. This size can even be small enough

for a few people to lift and deploy the AUV from a small inflatable boat, or even at a beach or boat ramp.

Regardless of size, role, or mission of the underwater vehicle, the overall design process is very similar and requires the iteration of the same engineering systems (Potter, *et al.*, 1992). The required onboard components can be divided into eight main groups (Healey and Good, 1992):

1. Containment System – Pressure vessels, hull structure, etc.
2. Energy System – Power supply, power management system
3. Mobility System – Main propulsor, through-body thrusters, control surfaces
4. Environment Awareness System – Depth sensor, conductivity sensor, thermometer, tilt sensors, accelerometers, etc.
5. Obstacle Avoidance, Navigation, and Guidance System – Sonar, GPS, compass, gyroscope, etc.
6. Autonomous Mission Planner/Replanner – Computer system and software
7. Failure Diagnostics and Error Recovery System – Releasable ballast, pinger, strobe light, etc.
8. Workpackage System – Sidescan sonar, sampling equipment, etc.

These components of the vehicle all need to be iterated in a complex design spiral, suggested by the following chart (Figure 2.4.2):

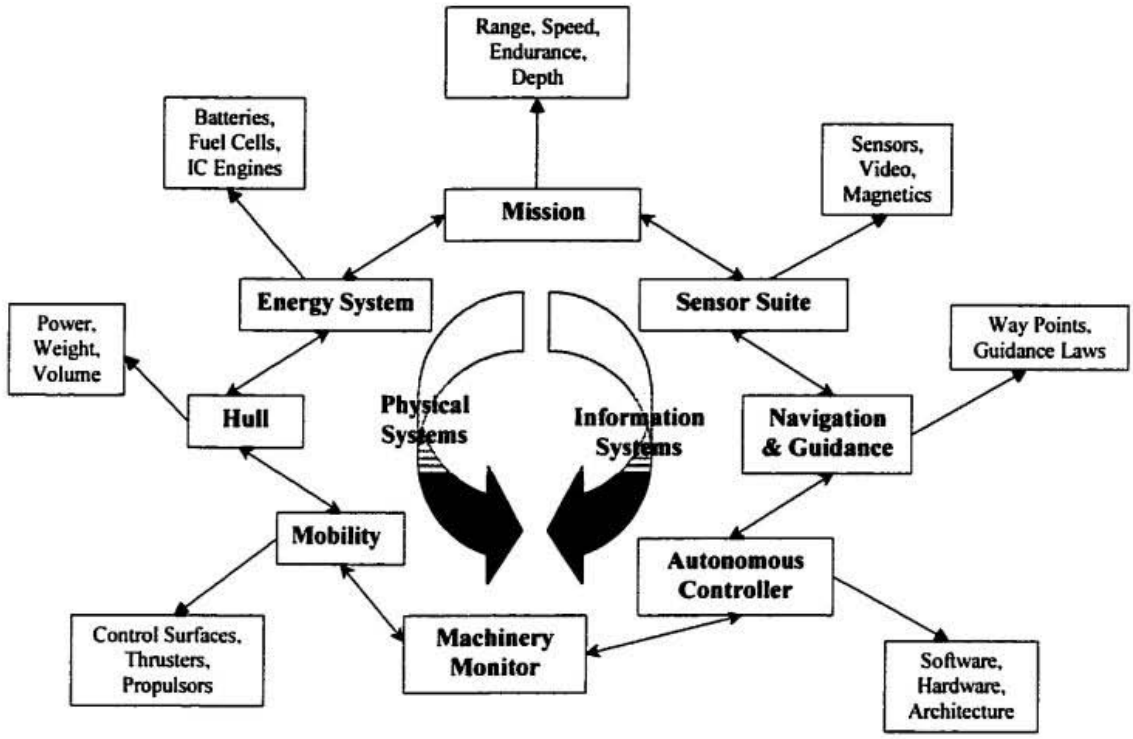

Figure 2.4.2: Integrated Design "Spiral" for an Autonomous Underwater Vehicle. Adapted from Healey and Good, 1992.

Chapter 3 – Detailed Design

3.1 THE C-SCOUT AUV

The designed AUV was named C-SCOUT – an acronym for Canadian Self-Contained Off-the-shelf Underwater Testbed. The original name for C-SCOUT was C-SCoUT where the "Co" referred to the word Contained. Early documents on the AUV reflect this. The name C-SCOUT describes the vehicle, its design, and purpose.

3.2 MODULARITY

To make the vehicle easily adaptable to a wide variety of configurations, the AUV was designed and constructed as simply as possible using modular sections. These sections allow lengthening and shortening of the vehicle to accommodate various payloads and control actuator configurations. The length of the parallel midbody can be adjusted based on the mission requirements to give the vehicle a maximum length of four metres. As the vehicle is free-flooding, except for a pressure vessel in the central module, adding modules does not require any sealing arrangements; it is just a matter of mechanical fastening with bolts.

Every effort was made to make each module neutrally buoyant and level in the water so that adding or removing a module does not effect the overall vehicle buoyancy and trim.

3.3 RANGE OF HULL CONFIGURATIONS

Since C-SCOUT is a modular AUV, a wide variety of configurations can be developed for specific missions or testing. Most planned configuration changes involve changing the number and type of actuators – for example, multiple sets of control surfaces could be used, or through-body thrusters could be added. For a local area survey vehicle, a skid could be added so the AUV could sit on the seabed and monitor the surroundings. To make C-SCOUT a versatile instrumentation package, a workpackage subsystem could be placed in one of the existing modules, or in an added module, depending upon the size of the package. These packages could include oceanographic data-collection equipment, sidescan sonar systems, underwater mass-spectrometers, explosives, debris markers, or even spools of fibre-optic telephone cable to lay along the sea floor.

The construction and testing of the vehicle was planned to be accomplished in stages. The Baseline Configuration of the vehicle has four control surfaces aft, and a single thruster aft for propulsion; see Figure 3.3.1. The length of this configuration is 2.7 metres with a hull diameter of 0.4 metres and an overall width and height of 1.06 metres from fin-tip to fin-tip.

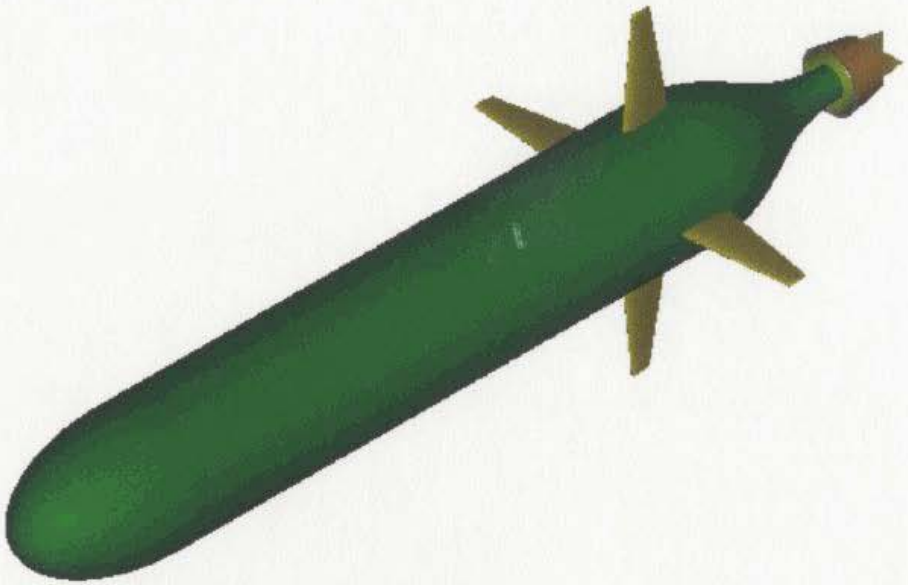

Figure 3.3.1: Baseline Configuration C-SCOUT AUV

The Fully-Actuated Configuration has the four aft control surfaces, plus four control surfaces forward of the center of gravity; see Figure 3.3.2. In addition, the Fully-Actuated version is to be equipped with six through-body thrusters. Two thrusters are to be placed vertically – one forward (A) and one aft (B), and the remaining four are to be placed horizontally – two forward (C,D) and two aft (E,F). The placement of the thrusters gives control in pitch, heave, yaw, roll, and sway, with surge control accomplished by the main propulsor, making the vehicle highly maneuverable even at low speeds and able to hover in a crosscurrent. The common practice is to use passive roll stabilization via gravity-buoyancy effects, but the Fully-Actuated Configuration C-SCOUT is designed to use thrusters so that it can maintain any orientation with ease, which may be necessary for underwater observations or data sampling. The Baseline Configuration, however, uses passive roll stabilization.

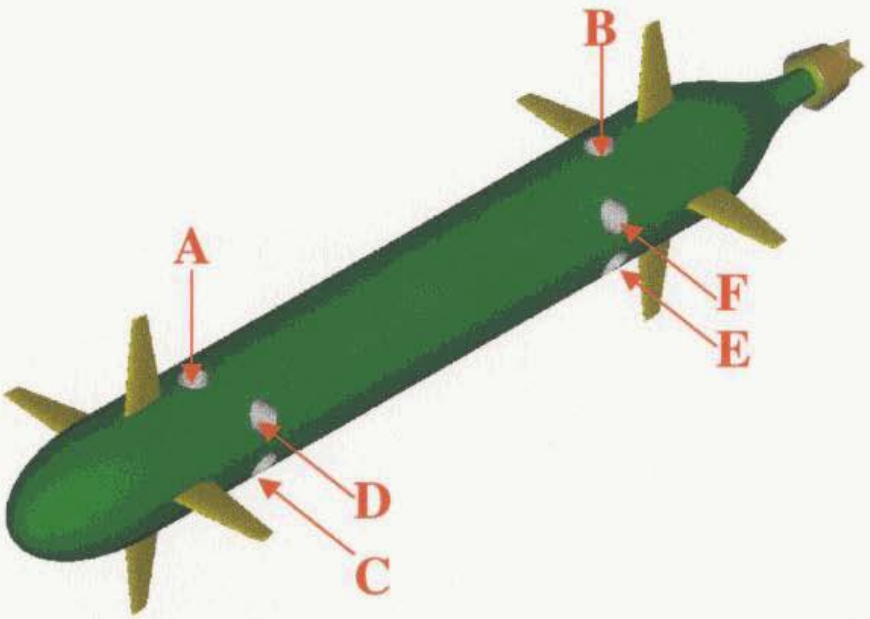

Figure 3.3.2: Fully-Actuated C-SCOUT AUV

Low speed maneuverability and hover capability are important in a cruising-type vehicle, such as the C-SCOUT, for sampling reasons. This vehicle could transit a considerable distance to a site of interest, such as an undersea plume, and then switch to low speed mode and monitor the site. Advanced modern sampling equipment that could be used to collect the information, such as an underwater mass-spectrometer, has a very slow sampling rate, which may be as low as one sample per minute or even less. A vehicle incapable of low speed maneuverability and/or hover would not be able to produce a realistic data map. Therefore, the C-SCOUT Fully-Actuated Configuration has real-world potential besides that of a testbed vehicle.

The overall dimensions of the vehicle were based on the components required onboard. These include an obstacle avoidance sonar, a computer system, a navigation and

orientation system, an energy-storage system, and a payload such as cameras or oceanographic sensors.

3.4 OVERALL VEHICLE PARTICULARS

Minimum Length (Baseline Configuration)	2.7 metres
Maximum Length (maneuverability limitation)	4 metres
Hull Diameter	0.4 metres
Overall Width and Height	1.06 metres
Design Speed (Baseline Configuration)	4.0 m/sec
Design Depth (test configuration)	10 metres
Endurance (with lead-acid batteries)	6 hours
Design Buoyancy (adjustable)	Neutral

3.5 C-SCOUT GENERAL ARRANGEMENT

Because the C-SCOUT AUV was designed to be as modular as possible, the onboard components that would be most consistent for each vehicle configuration were placed towards the center. This enabled simple switching of noses and tails without disturbing the power banks or computer system. Each module was designed to be neutrally buoyant so that reconfiguring the vehicle required only minor adjustments in buoyancy and trim. Also, each individual system was confined to a specific module to facilitate future

configuration changes. The general layout of the C-SCOUT AUV can be seen in Figure 3.5.1.

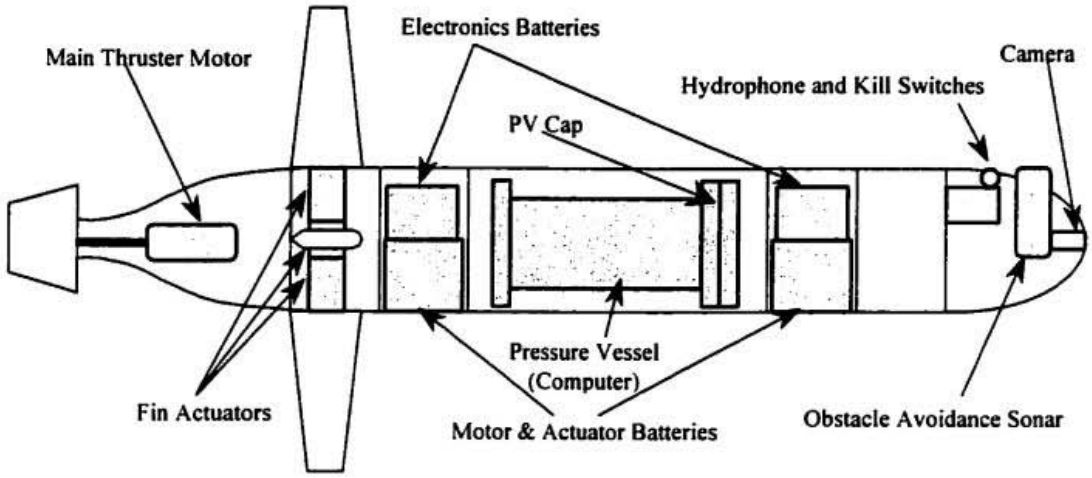

Figure 3.5.1: General arrangement of the C-SCOUT AUV

From the general arrangement, it can be seen that the pressure vessel cap faces forward – this was done because it was found to be significantly easier to drill holes for subsea connectors in a flat plate than in the end of the pressure vessel. Since most onboard sensors will be located towards the front of the vehicle, this design feature was built in to reduce future machining effort.

3.6 HULL FABRICATION

The vast majority of the AUV was made from aluminum alloy due to its light weight and high strength. The nose and tail of the vehicle, however, were constructed of glass fibre reinforced plastic (GRP) because of the complex curvature necessitated by streamlining the vehicle for good hydrodynamic properties. Manufacturing a complex shape out of

aluminum alloy would have been very costly and would require an advanced machine shop for any further modifications. By constructing them out of GRP, however, a mold was produced that could be used to quickly generate many more noses or tails (Figure 3.6.1). This is very useful in a modular sense since different propulsion systems, for example, can be housed in different tails and exchanged as needed.

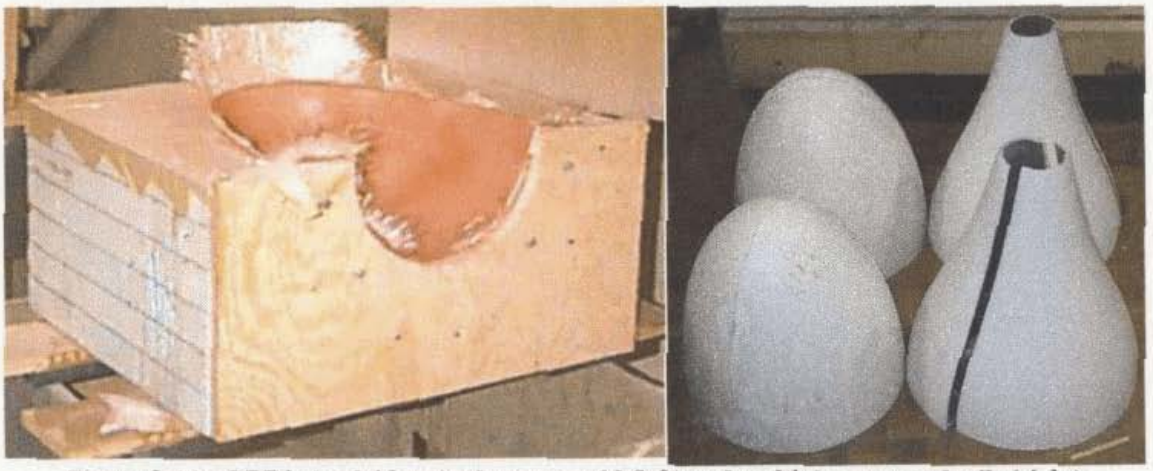

***Figure 3.6.1: GRP being laid up in the nose mold* (left) and multiple noses and tails (right)**

Using a simple flanged arrangement with nuts and bolts allows for imprecisely aligned modules to be pulled together by tightening the bolts (Figure 3.6.2). If a bolt were to become stripped or damaged in some way, it would be simple to replace it with no machining required. This method does require internal access to separate the modules, but that can easily be achieved by a split skin around the outside of the vehicle's hull. In this way, the top of the skin could be opened, exposing all of the internals of the vehicle and also allowing full access to the module separation bolts.

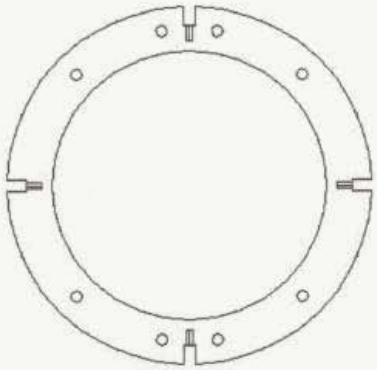

Figure 3.6.2: View of flanged module rings. The notches are for longitudinal stringer attachment, the two sets of two holes at the top and bottom are for instrument mounting, and the four remaining holes are to attach modules to one another.

The framework of the vehicle was designed for ease of manufacture and modification. Each aluminum alloy module is comprised of circular endrings with longitudinal stringers of flatbar connecting them and a thin aluminum alloy skin fastened around the circumference. The modules are joined to one another by heavy stainless steel bolts; see Figure 3.6.3. Refer to Boileau (1999) for complete detailed and dimensioned drawings of the C-SCOUT framework.

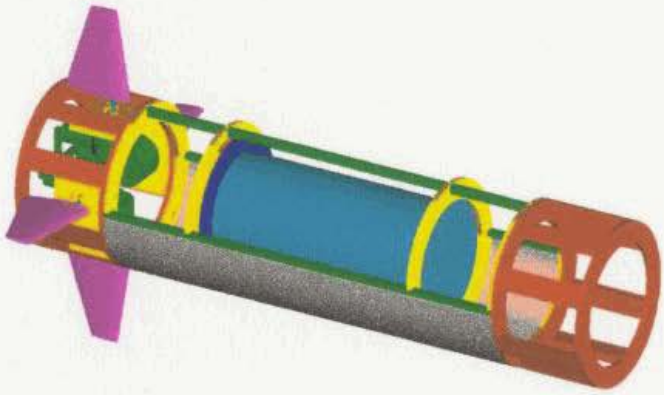

Figure 3.6.3: Cutaway of parallel midbody showing modular design

All of the endplates are manufactured exactly the same as one another, so that the only difference between each module is the length of the flatbar stringers and the skin. These stringers were fastened to the endplates using machine screws and can be removed to allow for recycling of parts into new modules. Therefore, for each new module, four pieces of flatbar have to be cut to the proper length, and have a hole drilled in each end. A new piece of skin would then be made to fit to complete the module. This process allows for very quick manufacturing that can be undertaken at nearly any machine shop (Figure 3.6.4).

Figure 3.6.4: Endplate milling (left), and assembled module before skin (right)

Structurally, the weakest link in the vehicle are the bolted stringer attachment points. However, structural calculations indicate that the entire *flooded* vehicle could be lifted by a single stringer in the current configuration. The vehicle is normally lifted by multiple

cradling slings that are placed underneath bulkheads though, so a large factor of safety is built in to the design.

C-SCOUT can be easily customized on a mission-by-mission basis. To change the entire look and functionality of the vehicle or to physically reconfigure it for a specific test, only requires undoing a handful of bolts and replacing or reorganizing modules as desired. While this is being done, the computer can be updated with the new mission- and configuration-based vehicle parameters to have the AUV ready to go as soon as possible.

3.7 POWERING OPTIONS

There are many options for power supplies for AUVs, but each one has the common goal of trying to maximize the endurance of the vehicle. Many experimental systems have been installed to lengthen voyage time. These include fuel cells, closed-cycle internal combustion engines, solar power, and ocean thermal energy power. The AUV DOLPHIN, built by International Submarine Engineering of Canada, is powered by a Diesel engine, but because it has a permanent snorkel, it is tied to the free surface. Tokyo University developed an AUV called the R-One that also has a Diesel engine on board, but it is closed-cycle and fed by a tank of liquid oxygen (URA Labs, 1995). All of the emissions are collected and recompressed so that the vehicle's buoyancy and trim are not disturbed as they would be if exhaust were released throughout the voyage. This

extremely complex and expensive prototype system, however, gives the vehicle a maximum cruising range of only 140 km, which is less than most conventionally-powered vehicles. For very long missions, it is expected that a closed-cycle Diesel engine will have a better power to weight ratio over battery systems. The initial overhead due to the engine becomes economical for long range because additional range can be achieved with an extra fuel tank, instead of extra banks of batteries. The system aboard the R-One is shown in Figure 3.7.1:

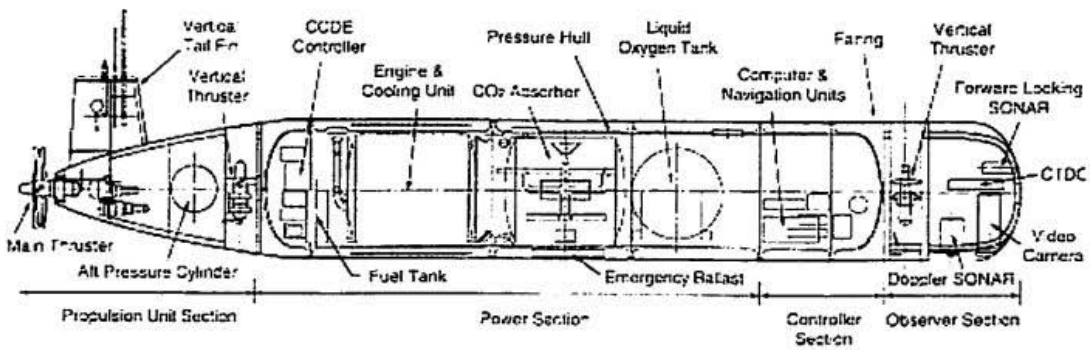

Figure 3.7.1: A diagrammatic view of the 8.2 metre-long Japanese AUV, R-One. Courtesy of URA Labs.

The Autonomous Undersea Systems Institute in New Hampshire developed an AUV that recharges its batteries with solar power cells while at sea (Marine Systems Engineering Laboratory, 2000). This is a way to acquire a longer range from a conventionally powered vehicle. Problems arise with this method, however, in trying to obtain a balance between necessary surface area for the solar panels, and a sensible size and shape for the vehicle. Their design is shown in Figure 3.7.2.

Figure 3.7.2: The Solar AUV, developed by the Autonomous Undersea Systems Institute of the United States. At the right, the solar panels have not yet been installed. (Courtesy of MSEL, 2000)

Another powering option is that used by the SLOCUM (Figure 3.7.3). This is an AUV developed in a joint project by the US Office of Naval Research, the Massachusetts Institute of Technology, the University of Washington, the Scripps Institute of Oceanography, the Woods Hole Oceanographic Institution, and the Webb Research Corporation. The goal of this heavily funded project was to develop an AUV with the longest possible range. To do this, a glider that changed buoyancy depending on external temperatures was developed. It will sink when warmed to ocean temperatures near the surface, and rise when cooled at deep ocean depths. The SLOCUM glides in a saw-tooth pattern at only a fraction of a knot, but it has a range of 40,000 kilometers over a five year period.

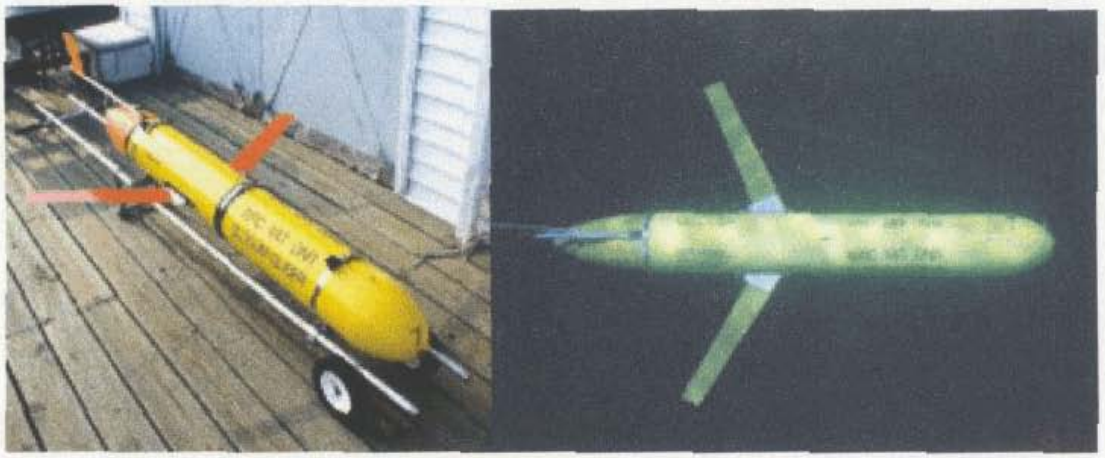

Figure 3.7.3: The ocean thermal energy powered SLOCUM has a range of 40,000 km over a period of 5 years. (Courtesy of Webb Research Corporation, 2001)

A vehicle powered by ocean thermal energy could be fully viable in the future, but very limited control is available for precision applications.

The most successful vehicles all use batteries, whether they be lead-acid, nickel-cadmium, alkaline, lithium ion, seawater, solid polymer, or the newer silver-zinc batteries that are found in cellular phones and laptop computers. These batteries are well proven, rechargeable, and readily available so multiple sets can easily be purchased to allow for one set to be recharged while the vehicle is still in operation. A comparison of the energy densities of the various types of batteries is shown in Figure 3.7.4.

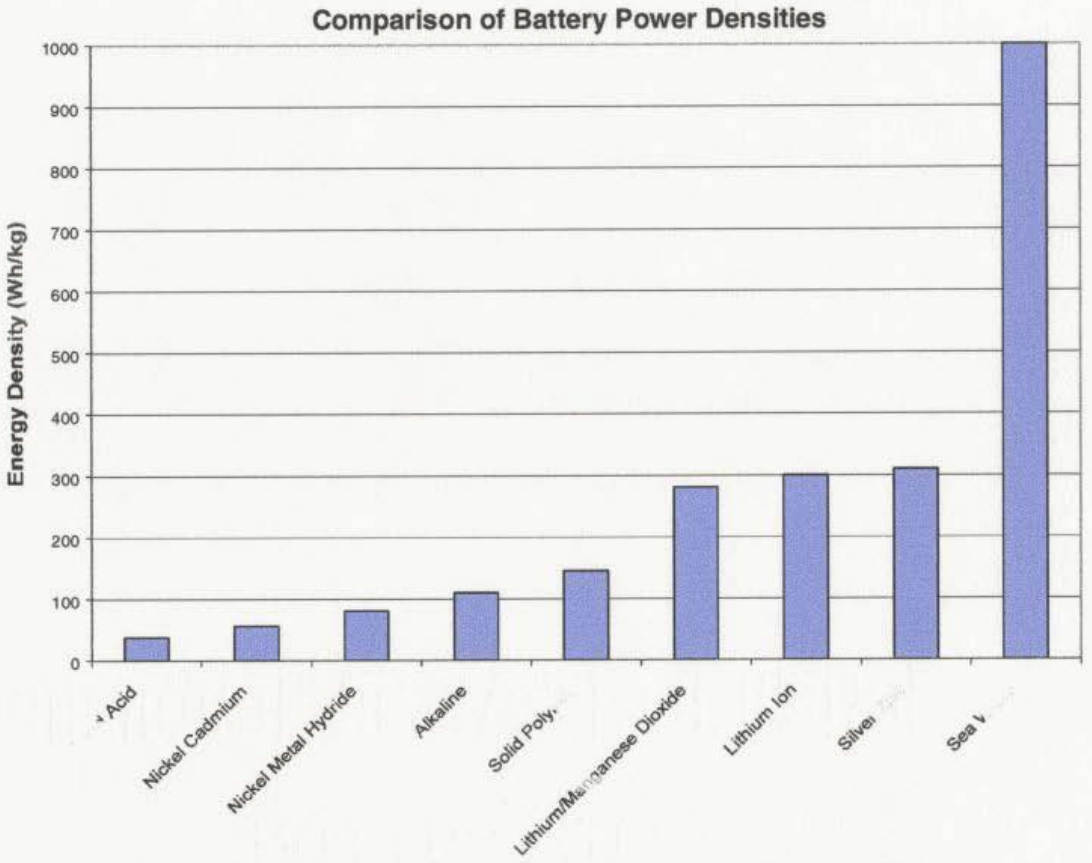

Figure 3.7.4: Comparison of available battery energy densities.

Currently, the C-SCOUT is powered by sealed lead-acid gel batteries because of their robustness, ease of use, availability, and low cost. For ocean use, the lead-acid batteries can be replaced by a source of much higher power density such as lithium ion, silver-zinc, or seawater batteries, fuel cells, or some other source. Upgrading from lead-acid batteries will give C-SCOUT a marked increase in mission endurance by a factor of ten or more, but will also increase the cost significantly.

Power is supplied to the vehicle from two separate banks of 12 volt sealed lead-acid gel batteries. The first bank of two 26.0 Ah batteries (312 Wh and 9.25 kg each) powers the computer hardware, and the larger second bank of four 31.6 Ah batteries (379.2 Wh and 11.0 kg each) powers heavier loads such as the main propulsor and the fin actuators. The total onboard power supply is 2.14 kWh with a weight of 62.4 kg resulting in a power density of 34.3 kWh/kg. The smaller batteries are those commonly found in emergency lighting systems, and are therefore very reliable and common. The larger batteries are actually motorized wheelchair batteries, which are also readily available and mass produced.

The batteries in C-SCOUT are placed external to the pressure vessel directly in contact with the surrounding water. Since the batteries have no pockets of gas inside them, they are incompressible and will be able to withstand the pressures due to the 10 metre maximum depth of the test tanks. However, during periods of excessive rates of discharge and sometimes during recharging, these batteries need to vent produced gases. Therefore, they are manufactured with simple one-way valves that open when the pressure inside is more than 1.5 psi above ambient. It is important to allow the batteries to vent to atmospheric pressure so that the batteries do not build up dangerous internal gases at high pressures. To overcome this problem, a Renshape™ box was built and sealed over the battery vents (See Figure 3.7.5).

Figure 3.7.5: Renshape box over battery vents. Note screw to allow venting during charging.

This Renshape™ box can withstand the water pressure and still allow the vents to activate properly, should this be necessary. A screw is threaded into each of these boxes and this must be removed during charging. Venting of the batteries has not been observed, nor should it ever happen with careful system use, but having the vents fully operational is a necessary safety factor.

Leads from the battery terminals were waterproofed with high quality Belzona 2221 MP Fluid Elastomer and attached to wet-pluggable underwater connectors. To reduce the out-of-water time of the vehicle, the batteries can be replaced very quickly and easily. This is accomplished by opening a hinged section of skin on the top of the vehicle to expose the batteries and watertight electrical connections. The batteries are mounted in trays and can be removed for recharging and then replaced with a fresh set.

For ocean testing, the lead-acid batteries should be replaced with a source of higher energy density, and the problem of venting should be solved. Batteries such as the solid polymer type do not need to vent and can therefore be placed exterior to a pressure hull, even in very deep water. Seawater batteries operate using magnesium anodes, seawater as the electrolyte, and oxygen dissolved in the sea water as the oxidant. They must be placed in direct contact with sea water in order to work, so many options are available for batteries placed external to a pressure vessel. According to Kongsberg-Simrad, these batteries are environmentally harmless, have a maintenance-free duty life of three to five years, an unlimited storage life, and have no danger involved in handling or in use (2001). They have a high initial cost, but to "recharge" the seawater batteries, the magnesium anodes can be simply replaced, even by an ROV, resulting in an overall low energy and downtime cost.

Chapter 4 – Design Calculations

4.1 PROPULSOR

The powering calculations (See Appendix A) suggested a single horsepower thruster (0.75 kW) would be sufficient to propel the baseline configuration at speeds up to eight knots, taking into account propeller losses and mechanical losses. Thrust deduction was estimated as 0.15. Two methods were used to estimate the drag of the vehicle – a method by Granville (1976) and a component buildup method by Nahon (1993). The Granville method is specifically tailored for underwater bodies, and corrects for nose shape, tail shape, parallel midbody, appendages, and surface roughness. Two estimates for drag were calculated using the Granville method – one based on a high surface roughness and one based on a low surface roughness. The component buildup method also accounts for most of the geometric variables in the various coefficients. The actual component buildup equations were taken from a program developed by the University of Victoria to predict data for the ARCS and Theseus AUVs, which are both torpedo-shaped like C-SCOUT.

The results of the calculations were very consistent with one another – the two Granville methods bounded the component buildup method, and the average of the two Granville methods was within five percent of the component buildup method (Figure 4.1.1).

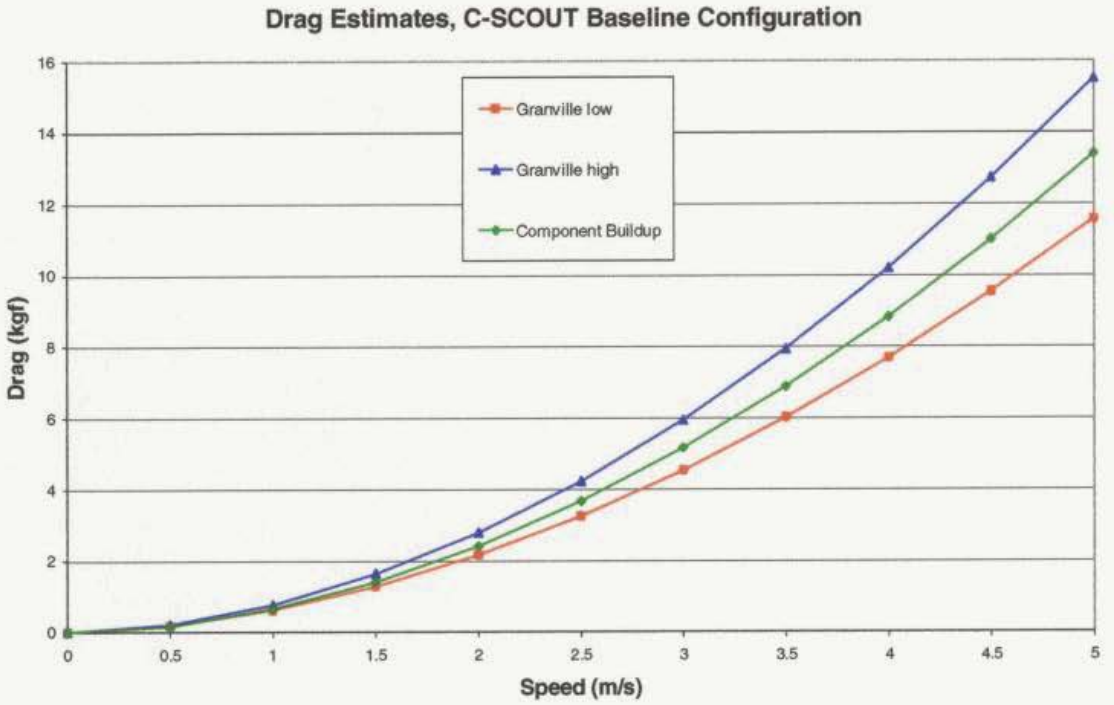

Figure 4.1.1: Predicted drag estimates for the C-SCOUT AUV Baseline Configuration

An integral off-the-shelf unit from Tecnadyne Advanced Product Development was selected that included the housed motor, shafting, magnetic coupling, propeller, propeller shroud, and flow straightening vanes (Figure 4.1.2).

It is important to note that the propeller is five-bladed. Since the vehicle will have a set of four fins, in a plus-sign configuration, a propeller with four blades should not be used. This is to reduce pulses throughout the vehicle as the blades simultaneously pass through the wake patterns of the four control surfaces. All of the available thrusters on the market require a high voltage so that current can be limited. The Tecnadyne 1020 Thruster needs 145 Volts, DC at 5.4 Amps, but to make it more compatible with the power system

aboard C-SCOUT, custom electronics were ordered to reduce the voltage to 48 volts while increasing the current to 15 Amps.

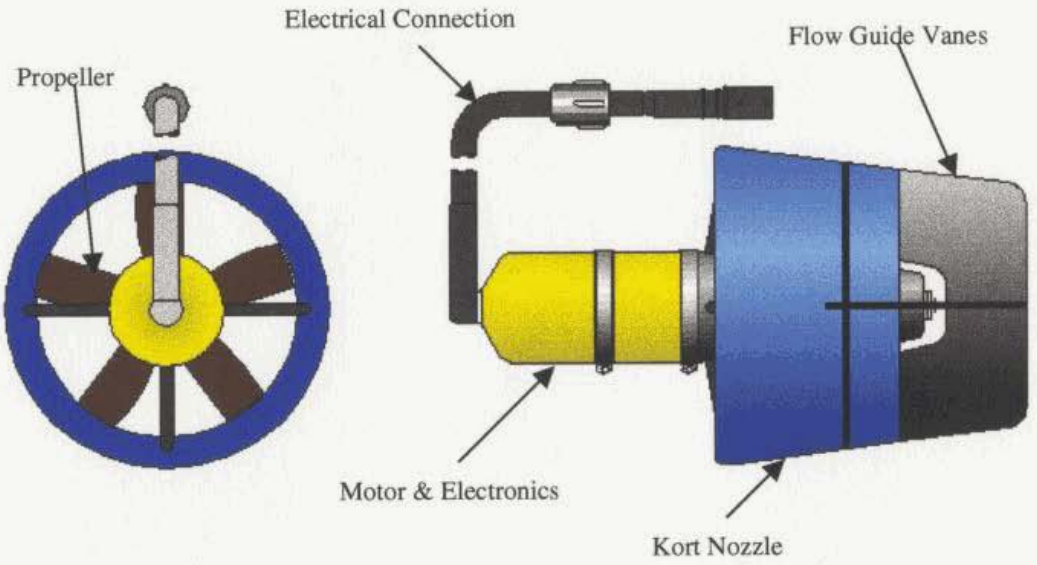

Figure 4.1.2: Model 1020 Thruster (1 horsepower, 6 inch diameter prop, approximate pitch of 0.70), manufactured by Tecnadyne Advanced Product Development. (Courtesy of Tecnadyne, 2001)

A representative from Tecnadyne said that detailed open water tests with the thruster unit have never been done, but tentative results claim a thrust decrease from bollard of 11% per knot of forward speed. The 1020 Thruster has 21.4 kg of forward thrust at bollard pull, so at eight knots, this would reduce to 8.4 kg of thrust. A comparison of this thrust reduction to the drag estimates for the C-SCOUT Baseline Configuration is shown in Figure 4.1.3. An estimated thrust deduction fraction of 0.15 is incorporated to give a better estimate of the performance of the thruster on the vehicle. A high estimate and low estimate for the Granville method are plotted, as well as the component buildup method.

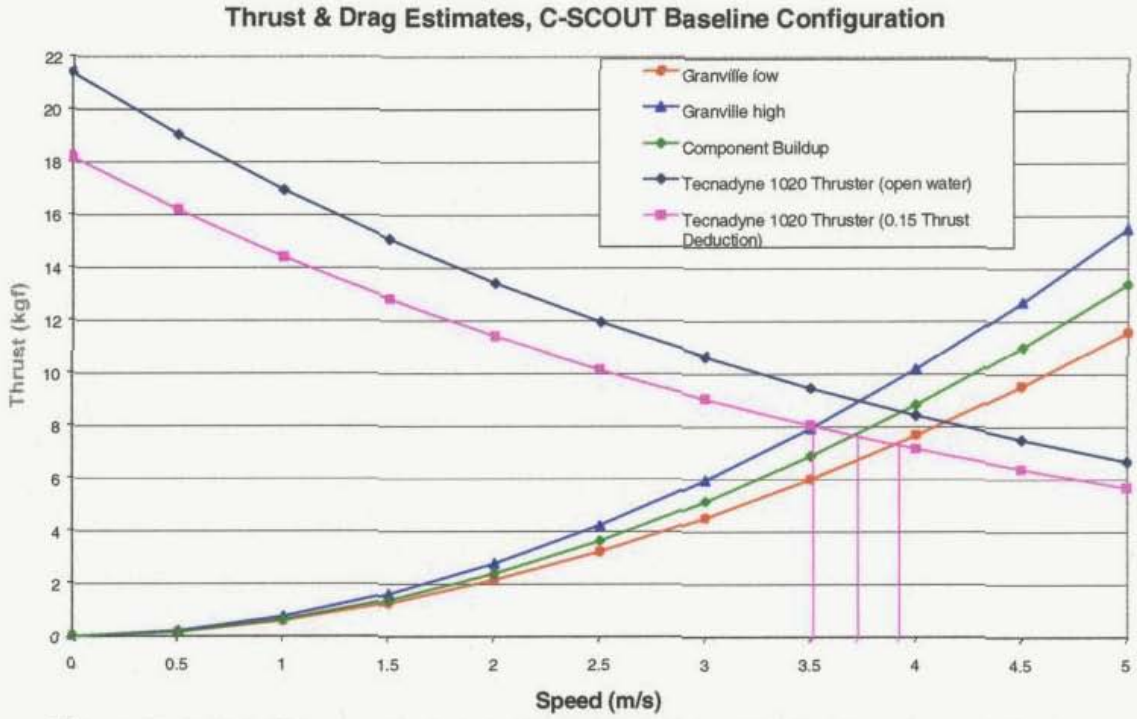

Figure 4.1.3: Plot of drag predictions for the C-SCOUT Baseline Configuration and thrust prediction for the Tecnadyne 1020 Thruster.

The intersections of the drag and thruster line (with a 0.15 thrust deduction) for vehicle velocity estimates are 6.84 knots (3.52 m/s) for the high Granville estimate, 7.18 knots (3.70 m/s) for the component buildup method, and 7.58 knots (3.10 m/s) for the low Granville estimate.

From the chart, this thruster is not able to propel the vehicle at the desired 4 m/s, but the next available larger off-the-shelf thruster was 2.5 horsepower, and therefore would have required considerably more battery energy storage. As the initially chosen speed was arbitrary, this thruster was used as a compromise. Future modifications to the vehicle

include developing more efficient propulsors that will be able to reach the chosen speed and work by Hermen Bijleveld on this topic was started in 2001.

Early problems were encountered with the Tecnadyne thruster due to back EMF (electric and magnetic fields) spikes. The motor armature on the brushless motors was made up of three low resistance, low inductance coils that were being alternately energized and discharged at approximately 13 kHz. In order to retain efficiency in the drive electronics, the power MOSFETs (Metal-Oxide Semiconductor Field-Effect Transistor) must switch this power very rapidly - slowing the switching down causes a lot of heat to be dissipated in the MOSFETs and limits the total amount of power to the motor. However, energizing the windings rapidly results in a very high leading edge current spike, as the power rushes into each coil. Similarly, discharging the coils results in a very high back EMF current spike that carries back onto the power bus.

In many ROV systems, that have a tether cable and power supply, there is sufficient energy storage in the system to effectively absorb these back EMF current spikes. However batteries are such a stiff power source that they are not able to effectively absorb the spikes. Therefore, it was necessary to provide a capacitor bank as close to the thrusters as physically possible. This capacitor bank was added after the initial problems with the system when motor electronics burned out.

While the Tecnadyne thruster was out of operation, a simple trolling motor was used as the main propulsor. The Minnkota 35T trolling motor, with the electronics assembly and connecting tube removed, was very easy to control since it was a brushed motor running at 12 volts. The motor, which is already waterproof, was mounted in the tail of C-SCOUT and the wire leads were waterproofed (See Figure 4.1.4).

Figure 4.1.4: Minnkota 35T Trolling Motor mounted in the tail of C-SCOUT with the two-bladed Weedless Wedge propeller attached.

According to the manufacturer, the trolling motor produced 12 kgf of bollard pull while consuming approximately 22 Amps. Stock propellers are available very cheaply that can propel the vehicle at typical trolling speeds. A two-bladed "Weedless Wedge" propeller, manufactured by Johnson Outdoors, was used for the initial in-water trials.

4.2 CONTROL SURFACE DESIGN

Since preliminary data, such as moments of inertia and radii of gyration, for the vehicle were not available at the design stage, empirical estimations had to be made to size the

control surfaces. Empirical methods using theory and then data correlations of systematic databases have been used in the design and analysis of over 150 undersea vehicles (Humphreys, 1994). The control surfaces were designed according to Det Norske Veritas rudder sizing rules for highly maneuverable ships (Landsberg *et al.*, 1983), including their suggested 30% increase in area margin for rudders in front of the propeller, and then increased by an additional 50% to match empirical data from other underwater vehicles (Healey and Good, 1992). The results of the calculations suggested an area of 330 cm^2 for each control surface would be required to achieve a turning diameter of approximately three vehicle lengths. Fins were designed with the desired taper ratio that had an area of approximately 358 cm^2. Appendix B contains the complete fin sizing calculations. The fins had a NACA 0015 section with an aspect ratio of three (ignoring the image effect at the root) with faired tips and a taper ratio of 0.40. The fins were tapered both at the leading edge and the trailing edge (Figure 4.2.1).

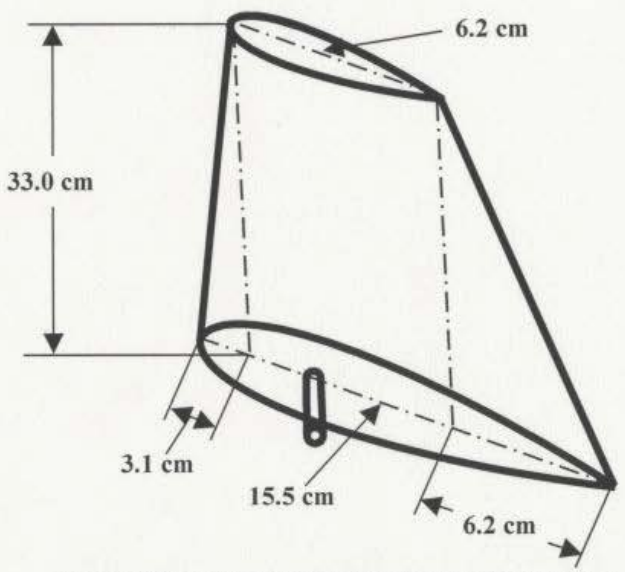

Figure 4.2.1: Control Surface Major Dimensions

The leading edge was tapered to reduce the chance of the vehicle snagging itself on a cable or a piece of seaweed, and the trailing edge was tapered accordingly to keep the quarter chord line perpendicular to the hull along the span of the fin. The quarter chord line is approximately the location of zero torque on the control surface, so by placing the actuator shaft along this line, the torque requirements of the actuator motors can be minimized.

The fins were attached to the actuators through a series of hollow shafts containing an internal shear pellet; see Figure 4.2.2.

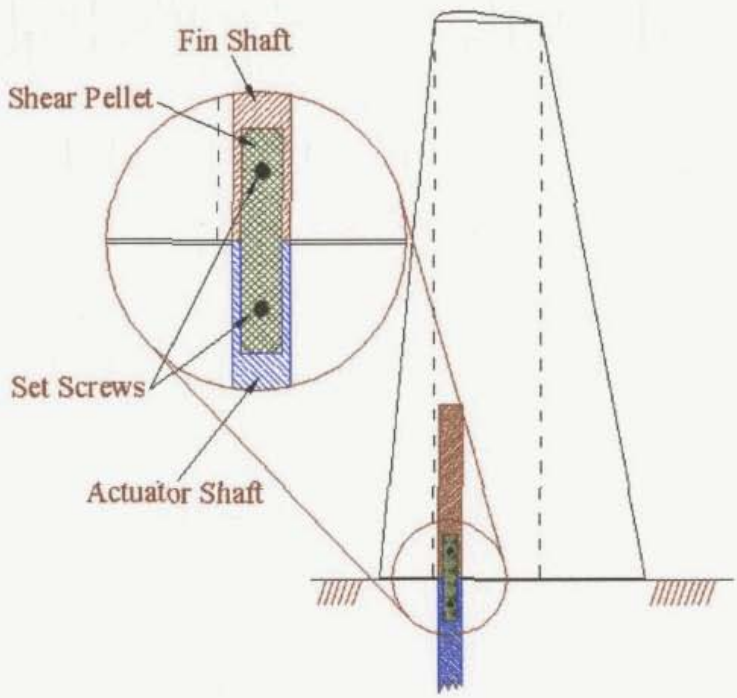

Figure 4.2.2: Control Surface Geometry and Attachment Scheme

This shear pellet is pinned inside the hollow shaft leading from the fin at one end, and is pinned inside the shaft leading from the actuator at the other end. In the event of a collision or permanent snagging of the fin, the shear pellet is designed to fail allowing the vehicle to swim free. Because of the "disposable" nature of the fins, they were cast out of epoxy resin in a mold making them very easy and inexpensive to manufacture (Figure 4.2.3).

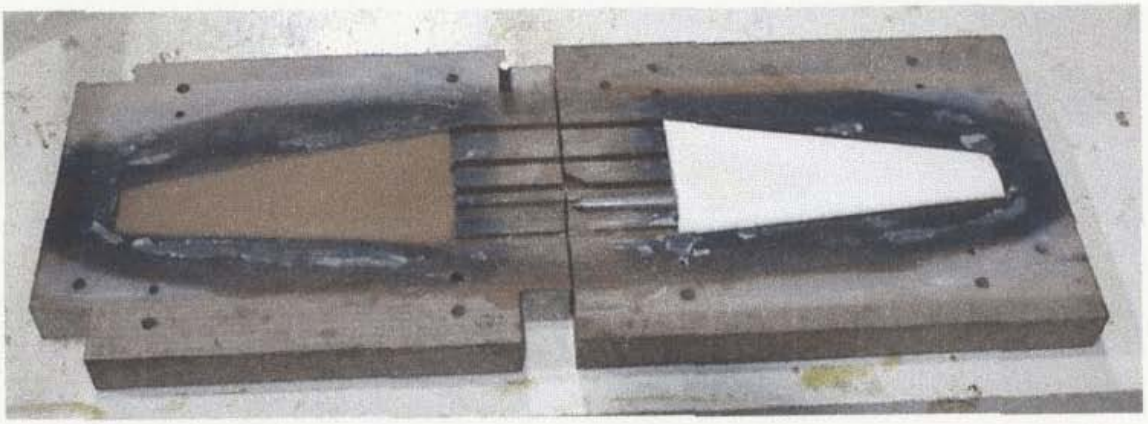

Figure 4.2.3: Mold for control surfaces – note dummy shaft in place to align fin shaft

The actual fin modules were sized and the actuators placed so that the fins could turn 180 degrees around and still fully overlap the parallel midbody for good flow characteristics. This was done to test vehicle performance in the reverse direction, as if it were backing out of a confined space such as a narrow channel or pipeline.

An additional degree of variation is achieved because of the bolting pattern between the modules; the fin modules can be used in the standard cruciform configuration (✦) or in an "X" configuration, allowing an even greater range of testbed capabilities.

The actuators used to control the fins are off-the-shelf motors in individual watertight aluminum housings. Stock waterproof actuators were available, but the cost was orders of magnitude higher than the custom waterproofed ones. The stock actuators cost nearly $8500 each, compared to $50 each for the electric motors. For a commercial vehicle designed for great depths and high reliability, purchasing these actuators is justifiable, but for the shallow depths C-SCOUT is intended to swim in the cost was prohibitive. To eliminate the issue of shaft alignment, the shaft seals were set in place using an elastomeric compound. The actuator housings can be seen in Figure 4.2.4.

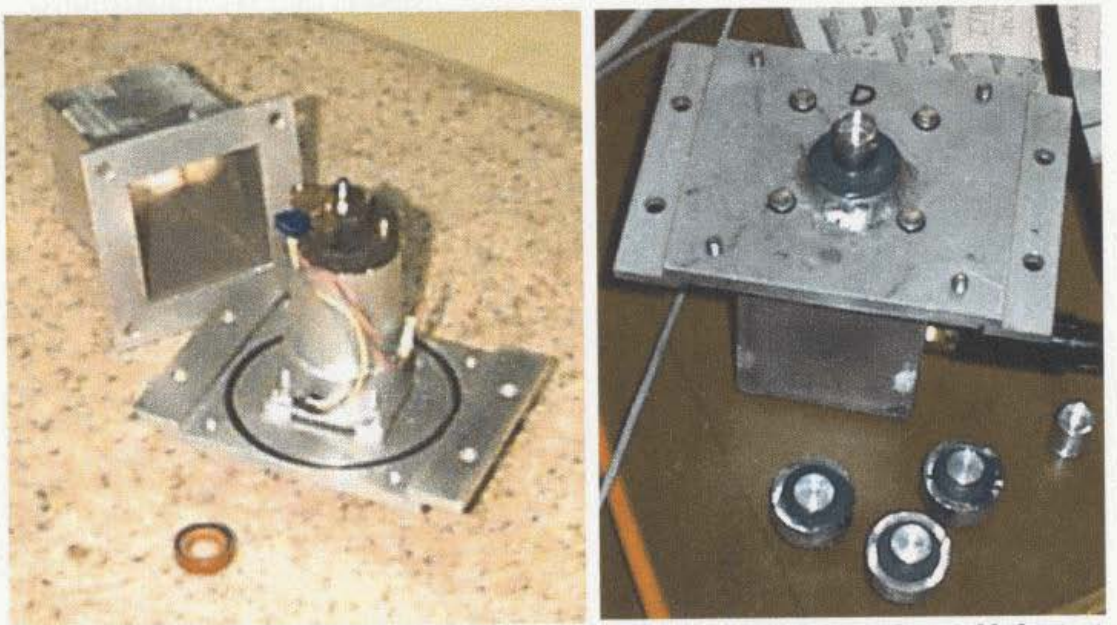

Figure 4.2.4: Actuator motor installed on faceplate with o-ring visible (left), and assembled actuator box (right) – note elastomeric compound used to seal the shaft.

4.3 PRESSURE VESSEL DESIGN

The options for designing the pressure vessel are to have it either as part of the hull, or to have it inside the hull. The advantage of an integral hull unit is that it allows for easier access to the interior if a top hatch is used. This would be a difficult hatch to manufacture, since it would need to make a three-dimensional curved seal, and then the latch mechanism would disrupt the fairness and symmetry of the hull. If an end hatch were used, like a lid on a cylinder, the vehicle would have to be dismantled into its modules before the pressure vessel could be accessed, and all cabling would have to run through the pressure walls.

If a separate pressure vessel were built and placed *inside* the hull, it could easily be removed by unfastening the skin sheet and disconnecting any cables. This quickly detachable skin would allow for pressure vessel removal in a matter of a few minutes by one person, since no heavy lifting, moving, or module alignment would be needed. This interior pressure vessel would also allow cables to be laid underneath it or around it without penetrating any pressure walls, but would reduce the amount of useable internal volume. With this method, the stress imposed on the vehicle during lifting operations or dynamic maneuvers will be taken up by the longitudinal girders, instead of by the pressure vessel walls. This reduced longitudinal strength requirement allows for much simpler construction since a simple aluminum pipe can be used instead of one modified with internal structures.

This section describes in detail the approach for designing a pressure vessel for the autonomous underwater vehicle C-SCOUT. The initial design is that of ease of construction, but in future designs, weight savings and increased depth are of utmost importance. The optimization of the pressure vessel is discussed with respect to weight at a particular depth, and this is compared to ease and cost of machining. The overall results provide a useful design chart for optimally designed pressure vessels with a lower bound of weight achievable for each particular depth. Also, a weight-depth optimization equation was developed and compared to the optimization routine results.

The design of pressure vessels has been a sector of engineering for many years, and various societies have developed governing rules and regulations. The majority of these methods all stem from basic mechanics principles and account for the various modes of failure for the vessel. One of the most commonly used methods is that developed by the American Society of Mechanical Engineers (ASME) for boiler pressure vessels. The results from the boiler code can be applied to any pressure vessel situation, regardless of whether external or internal pressure is applied. This code, or an adaptation of it, is commonly used in pressure vessel design for underwater vehicles.

The vehicle was designed to facilitate manufacturing and minimize costs, so all of the onboard systems and components are commercially available and the structural components are all standard sizes. In keeping with this methodology, the pressure vessel

was designed using readily available Schedule 40 aluminum pipe. The physical shape of the pressure vessel was chosen to be as simple as possible, even though it might not be the optimal shape from a weight-volume ratio standpoint. The shape for optimal weight-volume ratio is a sphere, or a chain of spheres. Spheres are very difficult to manufacture though, and are awkward to pack with computer equipment which tends to have squared edges. Therefore, a cylinder was used and the wall thickness was dictated by the required internal diameter to fit all of the computer components onboard. The internal length of the pressure vessel (minus the end caps) is 0.559 metres. The pressure vessel used is an unstiffened cylinder to reduce manufacturing costs for this first model of the vehicle, as it will spend most of its life in shallow (10 metre deep) test pools and not deep ocean environments. However, future versions are expected to reach many thousands of metres in depth to be used for exploration in the offshore oil and gas industry.

To eliminate the chance of galvanic corrosion, the pressure vessel had to be made out of the same materials as the rest of the vehicle – aluminum alloy. This made for a relatively lightweight structure with a great deal of strength and rigidity. Using more advanced materials, such as titanium, would dramatically cut down on the vehicle weight, but would increase the cost by orders of magnitude, and was not deemed to be a worthwhile tradeoff for the prototype vehicle.

There are three major modes of failure for pressure vessels under external pressure. These are yielding, buckling, and collapse (Allmendinger, 1990). The first failure mode

occurs when the extreme fibers at the outer surface and the inner surface of the shell undergo elastic yielding, which generally occurs at the mid-span between stiffeners or frames. The second failure mode occurs due to an elastic instability where the buckling occurs in inward and outward lobes to give a "dimpled" appearance. Collapse, the final mode, is caused by general instability of the shell and stiffener combination and results in a dished-in surface on the pressure vessel. Each of these failure modes are sensitive to particular criteria, such as cylinder shell thickness, length of unsupported shell, stiffener geometry, shell diameter, and material properties. By varying these parameters, pressure vessels can be adequately designed for each depth in question.

Since this project dealt with a pressure vessel designed for a particular application, all of the calculations used the constants listed in the following chart, and do not take into account the ends of the pressure vessel, as they can easily be constructed to withstand the maximum pressures by making them spherical.

Pressure Vessel Length	0.559 m	22.01 in
Pressure Vessel Internal Diameter	0.257 m	10.11 in
Yield Strength of Aluminum	$2.965*10^8$ Pa	43 kpsi
Modulus of Elasticity of Aluminum	$7.102*10^8$ Pa	103 kpsi
Poisson's Ratio for Aluminum	0.334	0.334
Density of Aluminum	$2.769*10^3$ kg/m^3	173 lb/ft^3

The detailed calculations are attached in Appendix C, but the methods and results are explained in the following paragraphs.

As a base example, the allowable depth for the currently manufactured pressure vessel that had a thickness of 0.792 cm with no additional stiffening is calculated. The results showed that the pressure vessel would collapse at approximately 320 metres depth and had a mass of 10.2 kg. By modifying this simple unsupported cylinder with a single 6.45 cm" cross-sectional area flat bar ring stiffener in the center, the depth rating could be increased to 1,485 metres, where the cylinder would buckle. For such a small addition of mass (total mass of 11.9 kg) and complexity, this is a significant increase in depth rating. The reason such a leap occurred is due to the change in failure modes. Unstiffened cylinders are very prone to collapse, whereas the ring-stiffened cylinders are very strong in that area, and therefore failure mode moves to buckling, which occurs at a significantly higher pressure.

Adding another of these ring stiffeners, to provide two equally spaced along the cylinder, increases the depth rating to 2,340 metres, where the pressure vessel fails in yield. The mass of this two ring stiffened pressure vessel is 13.56 kg, so again, a small increase in mass increased the possible depth dramatically. Adding a third ring stiffener increases the depth to 2,604 metres, and the mass to 15.23 kg, while the failure mode is still yield. Since yield is more a factor of the actual shell thickness, and not the stiffeners, an increase in the number of stiffeners at this point produces only a small gain in depth.

This pressure vessel is shown in Figure 4.3.1, where each colored point corresponds to a number of ring stiffeners, ranging from one to ten as shown by the pictures.

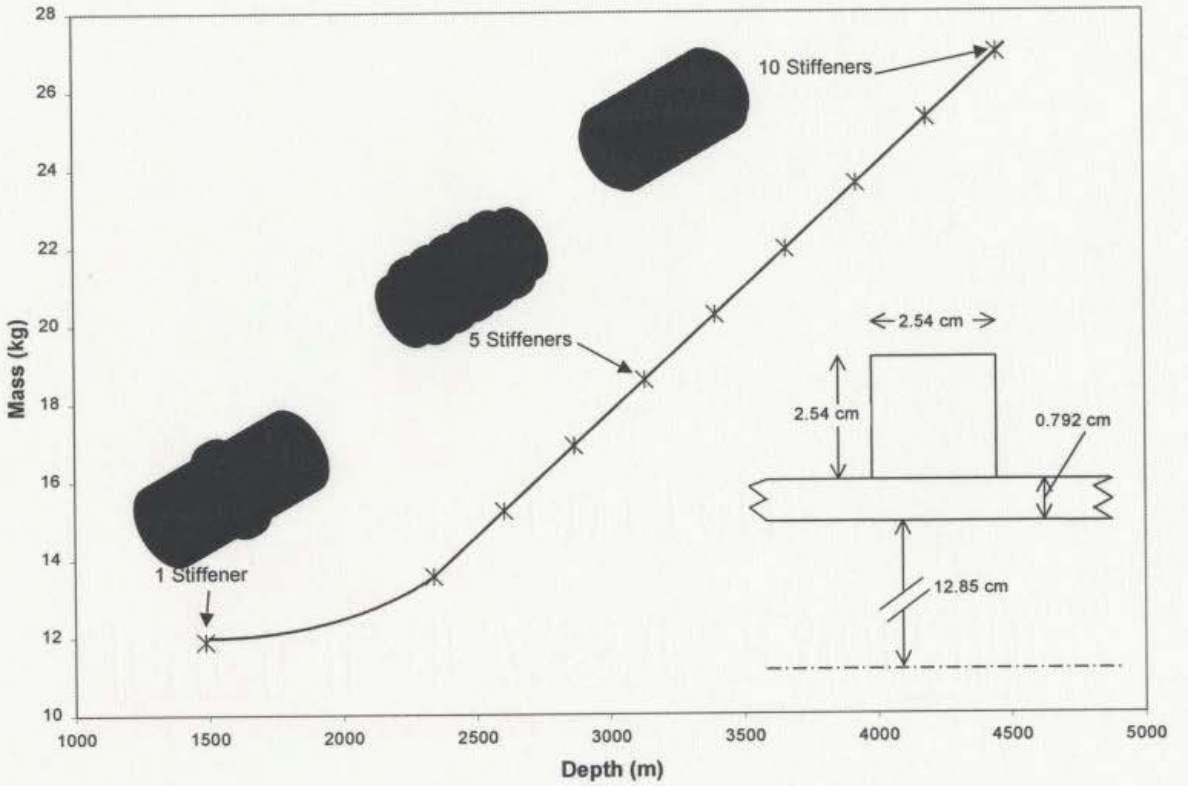

Figure 4.3.1: C-SCOUT pressure vessel with various numbers of simple ring stiffeners with cross-sectional area of 6.452 cm^2.

It can be seen from this graph how much of an increase can be achieved by the first few ring stiffeners during the changing failure methods, but then as the failure method becomes yield, the curve becomes linear. Similar results can be found by using other stiffener geometries on the existing pressure vessel shell. They each exhibit the same characteristic trend of changing failure modes, but some have a lower weight per maximum depth, while others have a lower manufacturing complexity per maximum

depth which is a tradeoff. In Figure 4.3.2, the immediate effect of the increased cross-sectional area and higher moment of inertia of a T-bar stiffener can be seen versus that of the flat bar in the graph above.

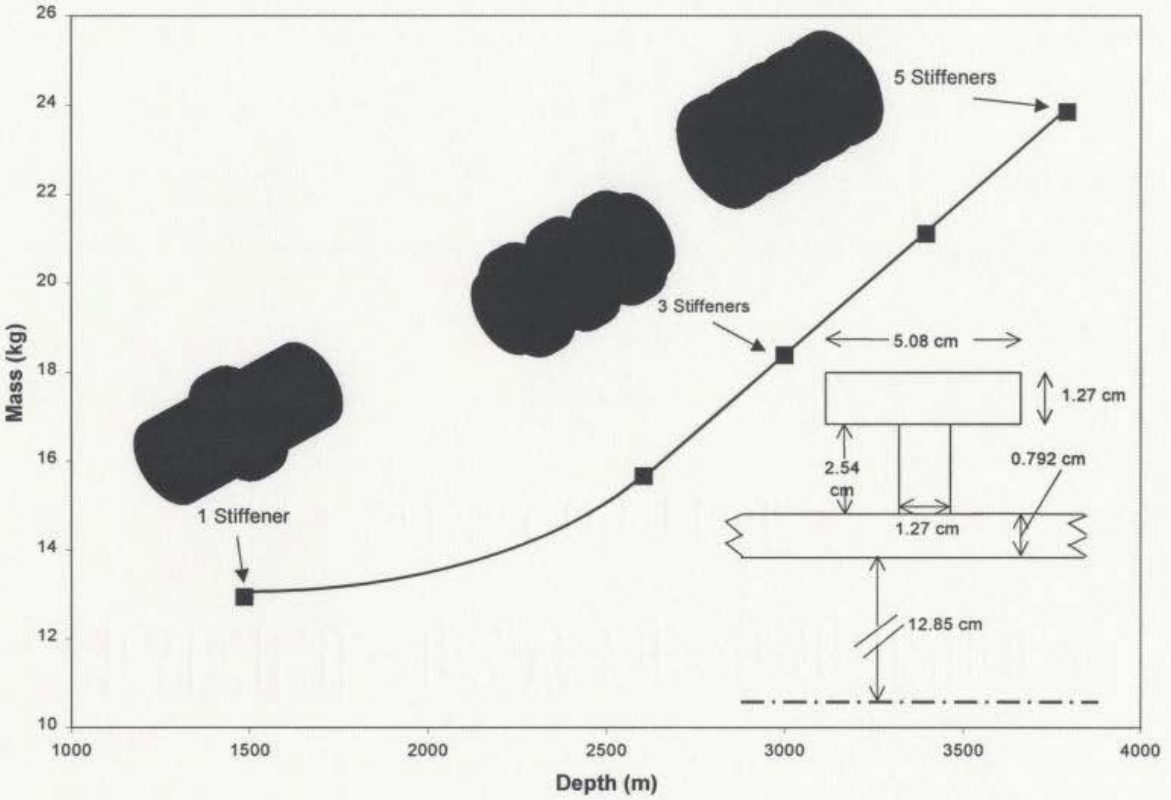

Figure 4.3.2: C-SCOUT pressure vessel with various numbers of T-bar stiffeners with cross-sectional area of 9.68 cm^2.

The increase in cross-sectional area of the stiffeners dramatically increases the initial weight, even though the same failure depth is reached. This is because the cylinder is failing due to the unsupported length, which is independent of the stiffener geometry – it is just affected by the number of stiffeners. When two of these T-bar stiffeners are used, the depth rating is 2,604 metres, with a weight of 15.66 kg. This can be compared to the flat bar design above, which also had a failure depth of 2,604 metres (coincidentally) with

three stiffeners, and a mass of 15.23 kg. Therefore, for a weight saving of less than half a kilogram (3%), but with an increase in ring manufacturing and welding of at least 150%, the same depth can be achieved. In this case, the small weight savings might not be worth the extra trouble of rolling and welding three rings, but on the other hand, it might be more advantageous depending on the method of construction of the T-bars. If the T-bar rings were constructed by using two separate pieces for each ring (a flange and a web), then four rings would have to be machined and welded instead of the three for the flat bar. The interesting point is that there are many ways to reach the same depth, and the most advantageous method would depend upon manufacturing techniques or stringent weight requirements.

Using a T-bar stiffener similar to the one used above, but with a double-wide flange on it markedly increases the moment of inertia of the ring stiffener and the area. The result is a much greater depth rating for added stiffeners (Figure 4.3.3).

The pressure vessel with two heavy T-bar stiffeners yields at a depth rating of 3,087 metres with a weight of 19.72 kg. This is a depth 18.5% greater than two stiffeners of the previous design, with a weight increase of 25.9%. Therefore, not a truly significant gain is achieved by this increase for only two stiffeners. As the number of stiffeners increase, however, a much deeper depth is achieved than with the smaller T-bar stiffeners.

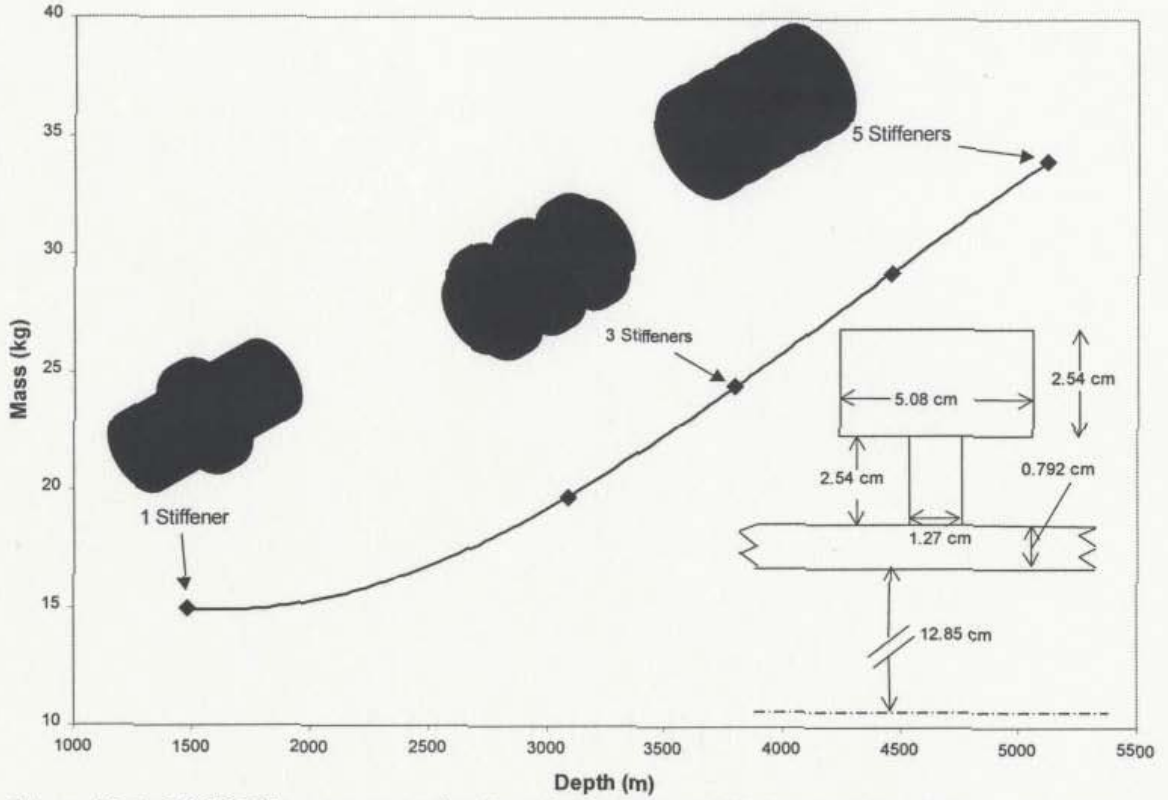

Figure 4.3.3: C-SCOUT pressure vessel with various numbers of T-bar stiffeners with cross-sectional area of 16.13 cm^2.

This large increase in depth capability can be attributed to the increase in cross-sectional area of the stiffeners, with no additional help from the moment of inertia of the stiffeners during the yield failure mode. Therefore, it is possible to design a stiffener with the same amount of area, but a lower moment of inertia. Generating a lower moment of inertia brings the majority of area (and therefore mass) closer to the center of the pressure vessel shell which gives it a smaller radius. Calculating the volume with a smaller radius yields an overall reduction of mass.

Using a triangular stiffener with the base attached to the pressure vessel shell of the same cross-sectional area (16.13 cm^2) as the large stiffeners above (to achieve the same depth rating) would decrease the moment of inertia of the stiffener and reduce the overall mass. The results are shown in Figure 4.3.4:

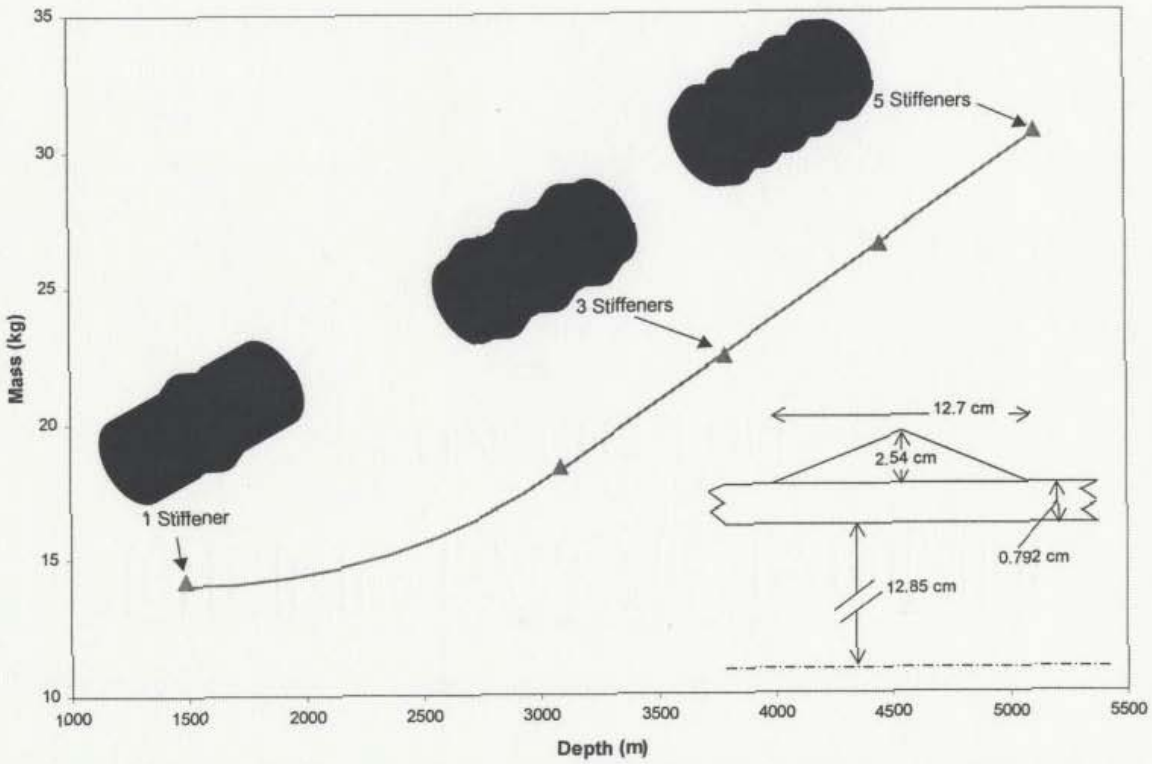

Figure 4.3.4: C-SCOUT pressure vessel with various numbers of triangular stiffeners with cross-sectional area of 16.13 cm^2.

Here, the same depths are achieved for each number of stiffeners as the wide-flange T-bar stiffeners, but the weight is lower. At the maximum depth, 5,112 metres, the weight for the T-bar stiffened pressure vessel is 33.99 kg, while the triangular stiffened one weighs 30.55 kg – a savings of over 11% for the same depth.

Figure 4.3.5 allows for quick comparisons between the various stiffener geometries. The individual data points still correspond to the number of stiffeners.

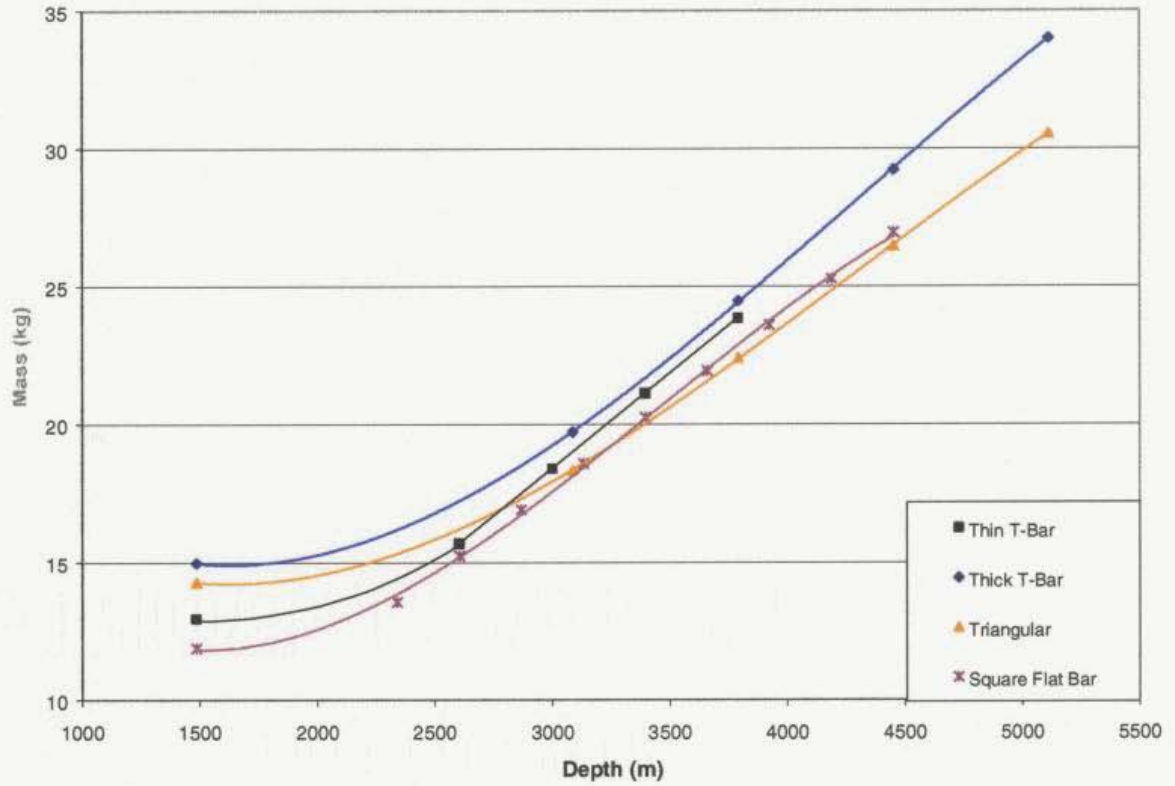

Figure 4.3.5: Effect of various stiffener geometries on the C-SCOUT pressure vessel.

Comparing the stiffeners in the chart above, it can be seen that there are cross-over points depending upon the desired depth. For example, at about 3,350 metres of depth, the triangular stiffener becomes more advantageous from a weight-savings standpoint than the square flat bar stiffener. At about 3,350 metres of depth, they are about equal in terms of weight, but there are five flat bar rings, yet only two triangular rings.

The above examples show the importance of the various factors involved in pressure vessel design. It is possible to solve for an optimal pressure vessel, in terms of weight to depth ratio, by successive iterations of the various failure modes. When the three failure modes occur at the same depth, then no single mode is overbuilt, and therefore the pressure vessel has the least for the depth. This idea is a continuation of the above method of reducing weight by lowering the moment of inertia of the stiffeners, since a high moment of inertia does not contribute to the strength of the pressure vessel in the critical region.

The failure modes can be brought together for flat bar stiffeners as follows:

1. Choose a cross-sectional area of the stiffener
2. Choose the number of stiffeners
3. Iterate the pressure vessel shell thickness until the local yield pressure and buckling pressure are equal
4. Iterate the number of circumferential lobes of failure (generally 1, 2, or 3) until the minimum critical pressure is achieved
5. Iterate the height to width ratio of the flat bar stiffener to change the moment of inertia until the critical pressure (collapse point) is equal to the yield pressure and buckling pressure
6. Check that the stiffeners do not overlap one another

This method yields a single pressure vessel design that is optimized for a particular depth. Each depth will have many possible pressure vessel designs – all depending on the

number of stiffeners and cross-sectional area of the stiffener. This is a very tedious process, and does not let the user choose the depth of interest. By completing many iterations, a depth close to that of interest can be achieved. A greater calculated depth should be used so that a factor of safety can be implemented.

The results from 17 such iterations are plotted in Figure 4.3.6 and show an interesting trend; the points of minimum pressure vessel mass for each depth are linear.

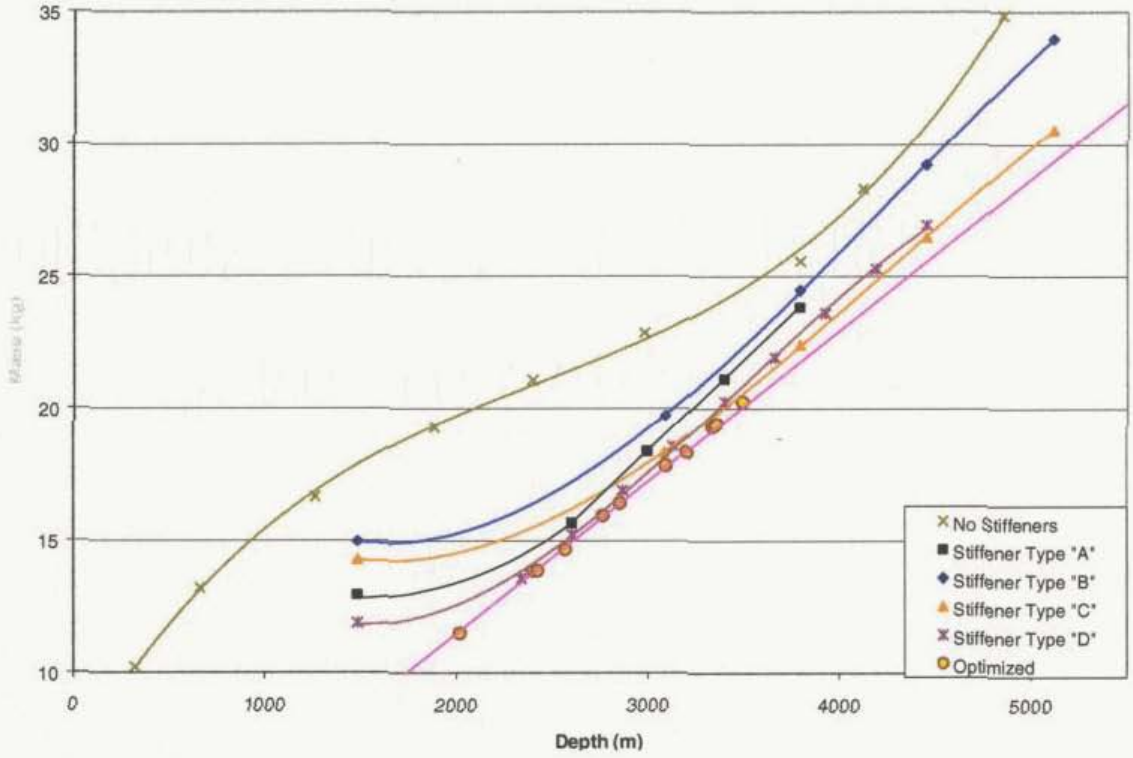

Figure 4.3.6: Pressure vessel optimization curve for the C-SCOUT AUV pressure vessel.

This is a lower bound curve for design, given the set length, internal radius, and materials used for the pressure vessel. A curve like this can be generated for any pressure vessel so that a designer can know the weight limitations for greater depths. If a greater depth was

required, but the additional weight was not acceptable, a different material would have to be used (for the same internal geometry).

There is no pattern of increasing stiffeners for deeper depths, or increasing individual stiffener cross-sectional area for deeper depths. The only correlation is the increase of the total longitudinal cross-sectional area along the length of the entire pressure vessel versus depth. The other parameters are all interrelated with one another – a decrease in the area of the stiffeners requires an increase in the number of stiffeners for the same depth, but it is insignificant which one is chosen from an optimization standpoint. As an example, an optimally designed pressure vessel for 1,555 metres of depth with four stiffeners of cross-sectional area 3.226 cm^2 each, requires a shell wall thickness of 0.449 centimetres, whereas one designed for a similar depth (1,562 metres) with three stiffeners of 3.226 cm^2 each requires a shell thickness of 0.51 centimetres. The loss of area due to the lower number of stiffeners is made up by an increase in the wall thickness for approximately the same depth. Figure 4.3.7 shows this very linear correlation.

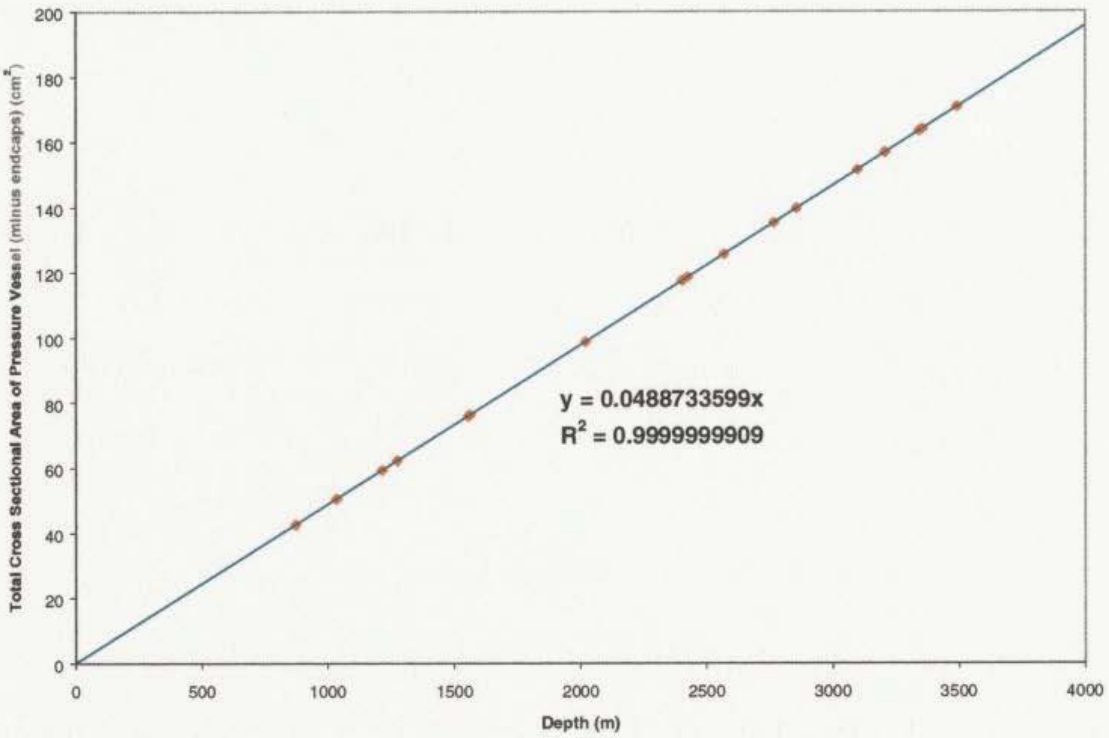

Figure 4.3.7: Correlation between pressure vessel cross-sectional area and achievable depth.

The reason the pressure vessel optimization curve and the above area curve turned out to be linear is because of the nature of failure. Recalling the earlier curves of sampled stiffener types, as the failure mode passed from buckling and collapse into the yield region, the curves exhibited a linear trend. For the optimized pressure vessels, all of the failure modes are brought to the same point, therefore they will all occur at the yield point. This causes the entire curve to be linear, and consequently, a linear relationship for the important parameters (total cross-sectional area in this case).

Knowing the lower bound is a very useful piece of knowledge, as it lets a designer know whether or not to accept the current design for a pressure vessel. The optimal curve uses

very precise shell thicknesses that would be unachievable in reality, with ring stiffeners of similar precision. As an example of this, an optimal pressure vessel to reach 2,857 metres has seven stiffeners of cross-sectional area 1.0 square inches (6.45 cm^2) each, with flange geometry of 7.0 centimetres in width and 0.923 centimetres high, and with a cylinder wall thickness of 0.441 centimetres weighing in at 16.415 kilograms. Manufacturing something like this would be a lot of effort, and nearly impossible to do. However, using the existing C-SCOUT pressure vessel thickness of 0.792 centimetres, and placing four inch-by-inch (2.54 cm x 2.54 cm) rings around it, a depth of 2,868 metres can be achieved with a weight of 16.91 kilograms. For these two vessels – one optimized, and one off-the-shelf, there is really little difference in weight for the remarkable difference in tolerances and complexity. If the optimal curve is interpolated at the specific depth of 2,868 kilograms, the resulting weight is less than half a kilogram different from the off-the-shelf pressure vessel.

The above example proves the usefulness of the design chart to show when it is worthwhile trying to optimize more, or if the simple design being used is acceptable. Figure 4.3.8 compares all of the pressure vessels designed, including the optimal ones, and also a curve for the case of unsupported cylinders of varying thicknesses.

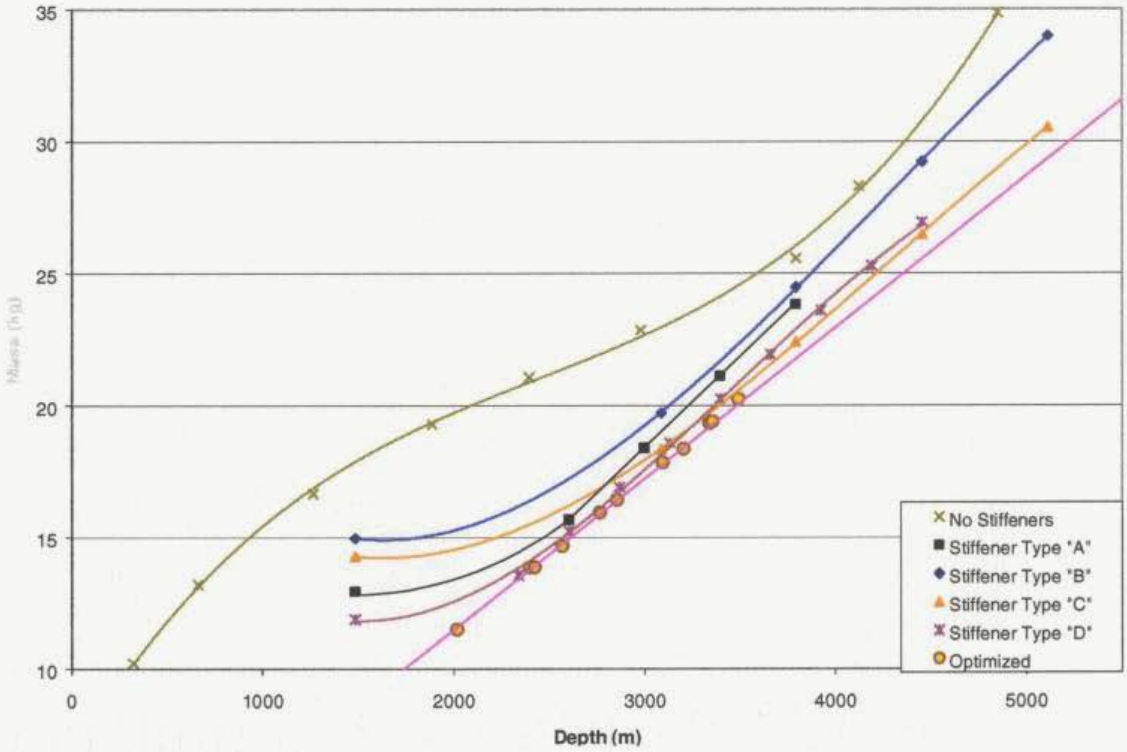

Figure 4.3.8: Effect of various stiffener arrangements on pressure vessel design.

From this, it can be seen how close some of the off-the-shelf pressure vessels come to the optimal curve. The non-optimized pressure vessel curves do not reach the shallower depths due to the constant thickness of the cylinder shell wall (0.792 cm). If a thinner pressure vessel shell were used, the curves would be closer to the optimal design at shallower depths, and a similar trend can be applied for deeper depths.

Although impractical from a machining and fabrication standpoint, the optimal design curve can allow for a comparison of various pressure vessels with respect to weight versus depth. The curve can also be used as a simple starting point for submersible design, as a pressure vessel need not be fully designed, nor specific details mandated for

a weight estimate to be achieved for preliminary hydrostatic calculations. From the standpoint of the C-SCOUT AUV, since it is designed with the simple unsupported pressure vessel in mind, the chart is useful in finding the maximum depth achievable without changing the size or material of the pressure vessel, or without a vehicle redesign. This depth is about 4,900 metres.

The equation developed from this study to estimate the minimum possible weight for a chosen depth is:

$$M = 2.9 \cdot \frac{L \cdot \rho}{\sigma_{ys}} \cdot R^2 \cdot d$$

where:

L = length (in)

ρ = material density (lb/in^3)

σ_{ys} = material yield strength (psi)

R = internal radius (in)

d = depth in saltwater (ft)

M = mass (lbs)

Or, in metric:

$$M = 0.0656 \cdot \frac{L \cdot \rho}{\sigma_{ys}} \cdot R^2 \cdot d$$

where:

L = length (cm)

ρ = material density (kg/m^3)

σ_{ys} = material yield strength (N/m^2)

R = internal radius (cm)

d = depth in saltwater (m)

M = mass (kg)

Figure 4.3.9 shows how well the equation matches with the optimization routine results for various lengths and radii.

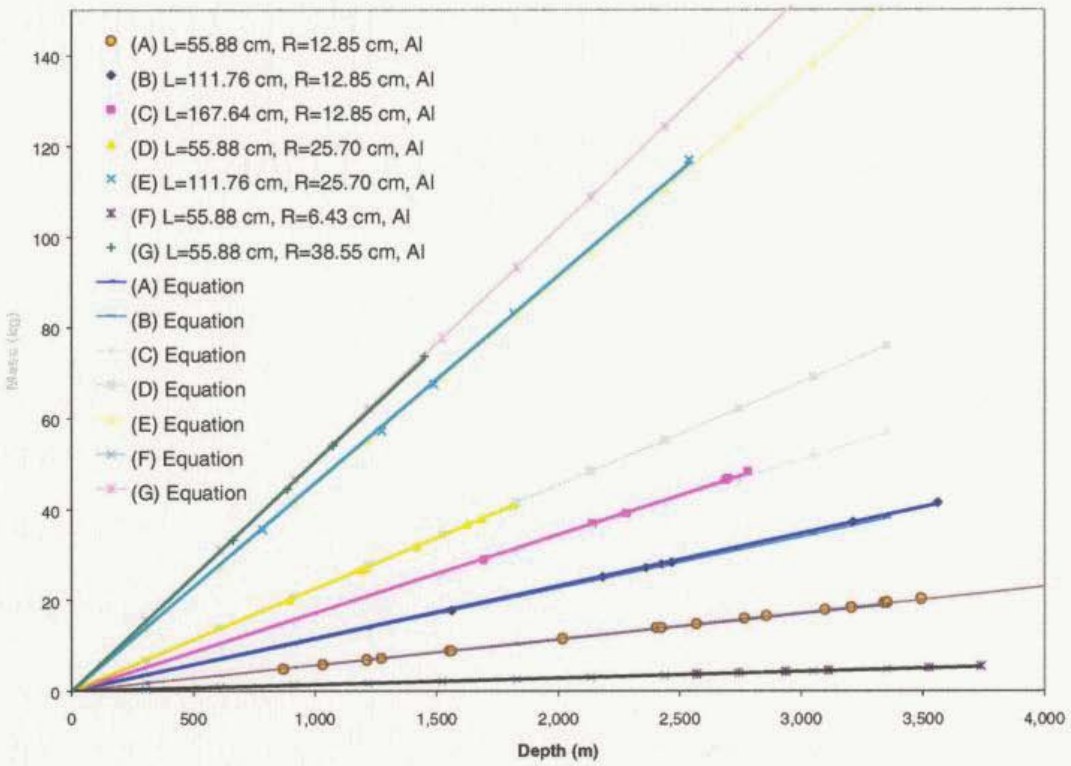

Figure 4.3.9: Comparison of pressure vessel weight versus depth for optimization routine and developed equation for various lengths and radii.

Figure 4.3.10 shows how the weight/depth ratio changes based on altering the material properties.

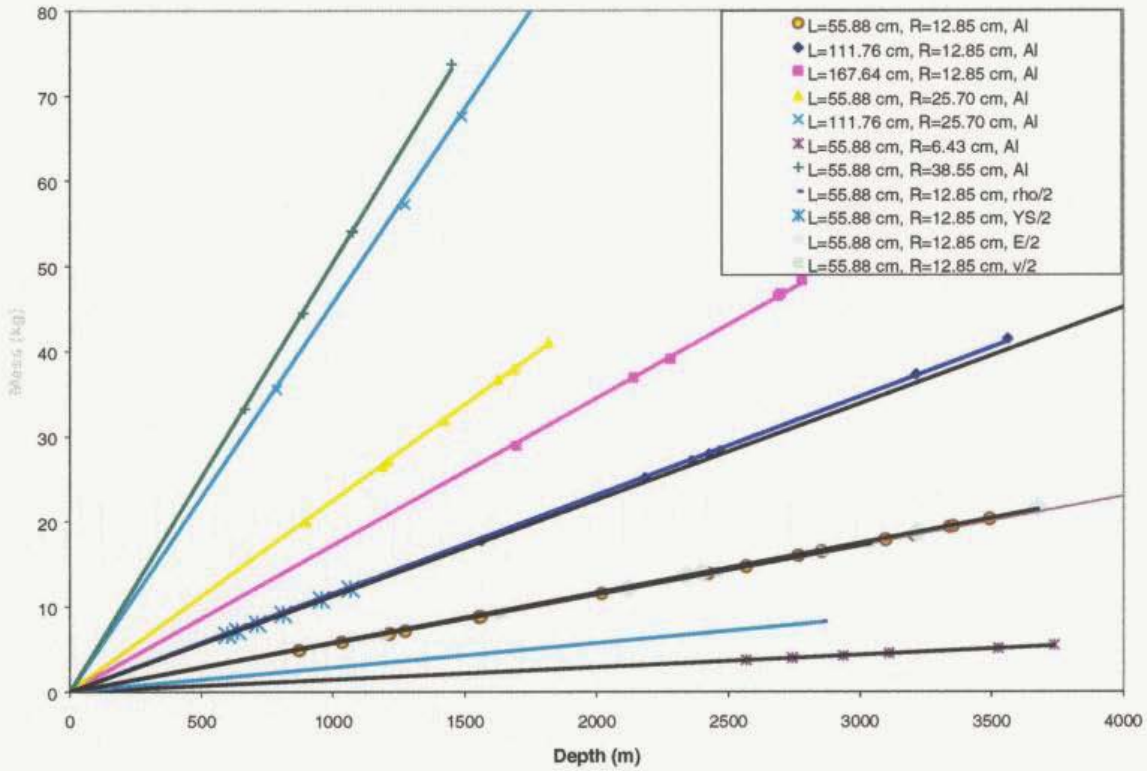

Figure 4.3.10: Comparison of pressure vessel weight versus depth for optimization routine and developed equation for various densities and yield strengths.

This equation seems to work well for the pressure vessel designed, for lengths up to three times longer, for diameters from a fourth the size to one and a half times the size, and for various material properties. The equation should also work for other, dramatically larger or smaller pressure vessels, but they have not been tried or tested. Therefore, caution should be used when applying the formula to a significantly larger pressure vessel. The

results of the equation can be used as a basis to rate various pressure vessel designs and compare them to the optimal design with respect to minimizing weight.

These depths are the designed maximum allowable depths, and do not take into account a factor of safety. A factor of safety must be included to account for manufacturing defects, warpage, material inconsistencies, unaccounted-for stress in the material, unforeseen impacts, or a variety of other reasons. The factor of safety can be lower for AUVs since there are no lives aboard so that in the chance of a catastrophic failure, only wiring and computers are lost.

An aluminum pipe of 10-inch nominal diameter (0.254 metre) and schedule 40, would have a minimum wall thickness of 0.312 inches (0.79 cm). This would allow the vehicle to descend to over 1,000 feet (305 m) before crushing. Therefore, the C-SCOUT pressure vessel was manufactured from a length of standard 10 inch nominal schedule 40 aluminum pipe with a bulkhead welded to one end, and a flange welded to the other. Dual O-rings and a series of bolts firmly seal the lid to the flange. This construction is significantly overdesigned for the relatively shallow operating depth of the test pools, but was simple to manufacture and can be used later for deeper ocean testing.

Chapter 5 – Onboard Systems

5.1 INTERNAL COMPONENTS

The onboard components were arranged to minimize the electrical interference with one another. Most of the electronic components were housed inside the pressure vessel; some instruments to be added later, such as the compass, should be housed in their own pressure vessels shielded from any electrically generated magnetic fields. The electronics components inside the pressure vessel were mounted on a sliding chassis that can be removed as a unit to facilitate access to them (See Figure 5.1.1). This chassis provided a solid mounting surface for the electronics, and also doubled as an effective heat sink for the motor amplifiers which run hot.

Figure 5.1.1: Chassis to mount electronic components (left), shown sliding into pressure vessel (right).

5.2 COMPUTER SYSTEM

The vehicle's primary systems are the computer system, power supply, navigation and positioning system, a sensory system, and an emergency response system. The computer system was made up of a Pentium II 266 MHz microprocessor using PC-104 technology for input/output functions. A Microsoft Windows NT operating system was utilized so that Windows-based programs could be employed for the development of control algorithms. Data collected during the vehicle's mission can be stored on an onboard hard-drive for subsequent retrieval and processing. The selected navigation and positioning system was a KVH GyroTrac system to find magnetic and true north, roll, and pitch angles. A Tritech SeaPrince obstacle avoidance sonar was mounted in the nose to detect nearby objects so that the AUV could alter course or depth to avoid a collision. For the initial testing of the vehicle, the sonar was mounted on the top of the nose (See Figure 5.2.1). This mounting arrangement was chosen to protect the sonar head in the event of a nose dive during early testing. Since the test tanks have a known flat bottom without any obstacles, the AUV does not need to look down. For testing in a natural environment, however, the nose can be inverted so that the sonar can see objects below and in front of the vehicle.

Some of the other onboard sensors include a depth sensor, a hydrophone, a camera, and a payload. The depth sensor is mounted inside a heavy bolt, which is screwed into one of

the pressure vessel bulkheads. This mounting arrangement was chosen so that pressure sensors of different range and accuracy could be mounted in a standard size of bolt and swapped out easily. The hydrophone is mounted on the top of the vehicle in the nose module just aft of the sonar, and listens for a particular signal to abort the mission and return to the surface. A small, waterproof, black and white streaming video camera was mounted directly in the nose. This camera was able to take still pictures or video feed.

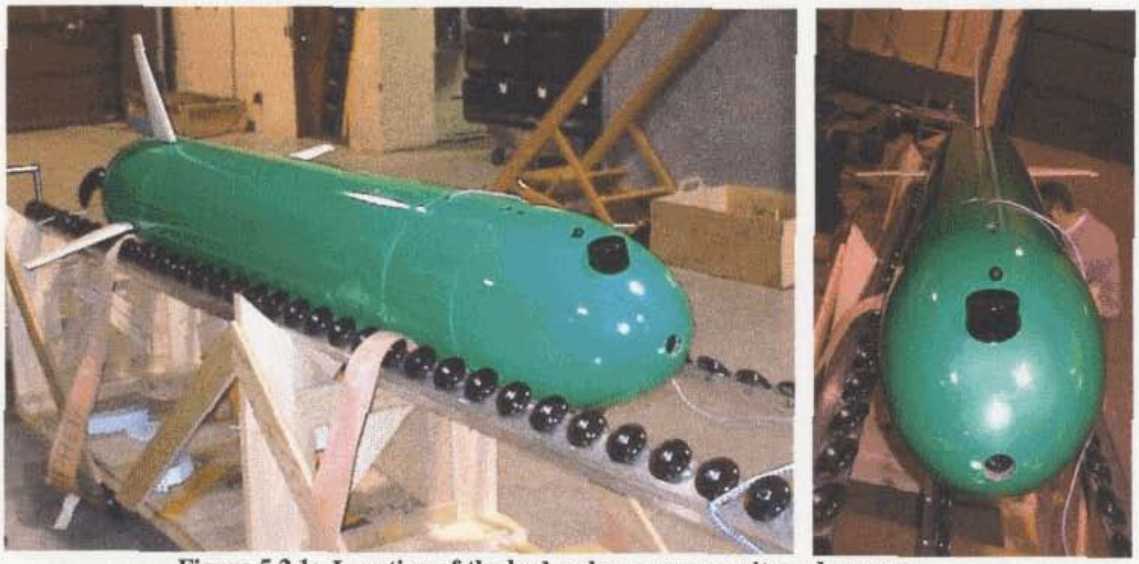

Figure 5.2.1: Location of the hydrophone, sonar unit, and camera.

The initial testing phase involved determining the preliminary capabilities of the vehicle. During these initial tests, the vehicle communicated with a supervisory computer by an Ethernet umbilical cable so that data could be exchanged between the AUV and the observers.

The only watertight section of the hull is the internal pressure vessel, which houses the computer system. The other components are spread throughout the hull, each individually waterproofed and attached using subsea connectors. The connectors are from Subconn Underwater Connectors, and are all rated to either 10,000 psi or 20,000 psi (23,000 feet or 46,000 feet of fresh water). The connectors are screwed into threaded holes in the bulkheads and seal with a single o-ring. All undersea connectors require a substantial amount of physical space, but the Subconn series are the smallest and most robust. The initial design length of the central module had to be lengthened by several inches to accommodate the underwater connectors. The connectors are lubricated with standard silicone grease to make them easy to connect and disconnect. Delrin™ locking sleeves were attached to the fin actuator connectors because they are more of a permanent fixture than the connectors attached to the pressure vessel.

There is room around the pressure vessel for cables to be run from nose to tail, and there are small tunnels between the batteries for cables to pass (See Figure 5.2.2). Excess cable length can be coiled up in the space around the connectors at the ends of the pressure vessel. The connectors were chosen such that it is impossible to plug in the wrong connectors by way of combinations of connector size, number of pins, and male/female composition.

Figure 5.2.2: View of stacked batteries showing cable tunnel.

The battery modules are clustered around the pressure vessel so that they are near the center of the vehicle to reduce cable running and also to evenly distribute weight placement. Weight placement is very important since the battery modules are one of the heaviest components in the vehicle. The fin modules are placed as far forward and aft as possible so that the fins can be small in size and can still generate the required steering moment. The fin modules are as short as possible, leaving enough room to fit in a motor, without the fins hanging over the curved nose and tail. The tail is faired into the motor housing to allow good inflow to the propeller.

C-SCOUT was painted marine grade fluorescent green to make it easy to spot, even at depth. Color is attenuated in water, starting with the red end of the spectrum and moving towards the blue end. Brilliant red on the surface will appear dull brown 10 metres under the water. Bright green will remain bright green even hundreds of metres below the

possibly shallow local lakes and bays, a highly visible color is required. If C-SCOUT were to become trapped or have a failure for some reason and sink to the bottom, the bright green hull would be relatively easy to find by a diver, whereas a red hull would camouflage the vehicle in the dark brown mud common to these parts of Newfoundland. For ocean testing, however, high-visibility red or orange stripes should be painted on the vehicle to help spot it on the sea surface.

5.3 FLOTATION

Since C-SCOUT is free-flooding, there is a need to add buoyancy material to bring it to a neutrally buoyant stage. Deepwater flotation is readily available from companies that supply ROV flotation, and this can be machined to any shape and is strong enough to be used as a mounting surface for equipment or sensors. For the initial testing, buying and machining this relatively expensive foam is impractical since the arrangement of onboard components changes so often, as does the overall weight and therefore buoyancy requirements of the vehicle.

For the shallow pool testing planned for C-SCOUT, standard household Syrofoam® foam insulation can be used. This foam is purchased in large sheets and is used at IMD to construct the hull forms that are tested in the tanks. Therefore, plenty of scrap was available to cut into custom-fitting blocks for C-SCOUT. It is very easy to add another chunk of foam or shave one down to achieve close to neutral buoyancy. Over time, however, small changes in buoyancy due to leaks in the actuators or the release of

however, small changes in buoyancy due to leaks in the actuators or the release of trapped air bubbles cause the vehicle to slowly sink. It is evident that some form of adjustable ballast and trim system is required in future tests to compensate for these changes and other dynamic changes that occur due to water density.

Holes were drilled along the upper and lower surfaces of the vehicle to allow water and air to flow in and out during deployment and retrieval (See Figure 5.3.1). The holes are larger on the bottom so that the vehicle will flood and drain rapidly. It is important to shake the vehicle back and forth as much as possible once submerged to try and get all of the tiny trapped air bubbles loose.

Figure 5.3.1: Air and water drainage holes. Holes on top are small (left) for allowing air in and out, while those on the bottom are much larger (right) to allow water to freely drain in and out.

5.4 CONTROL SYSTEM

AUVs have a control system loaded into their computers to define their behavioral characteristics as well as their mission parameters, waypoints, etc. C-SCOUT does not yet have an autonomous control system, so it is controlled through an umbilical or by radio communication. The other end of the umbilical or radio transmitter/receiver is connected to a laptop computer running the Symantec "PC Anywhere" software. This allows a user to view the screen that the C-SCOUT computer would see, and operate the vehicle accordingly. Near-real time data can be transmitted in this fashion with only minor coding and software development.

5.5 NAVIGATION SYSTEM PLANNED FOR FUTURE TESTING

There are various methods for firmly establishing the location of an autonomous underwater vehicle. The most definite way is to use a baseline positioning system, with buoys that send out signals from precisely known locations. The signals are used by the AUV as positioning vectors. A buoy system of this configuration is precise, and it would be superb for a stationary site, such as an offshore platform, a shipwreck, or a geothermal vent. This system is not appropriate for missions that cover more than half a mile, or for rapid deployment of AUVs without initial setup time. Another precise system uses a Differential Global Positioning System (DGPS) for the AUV to locate itself. DGPS is used by vehicles that never leave the surface, such as the DOLPHIN (Figure 5.5.1),

because the water attenuates the signals, and therefore they cannot penetrate the water for more than a few feet.

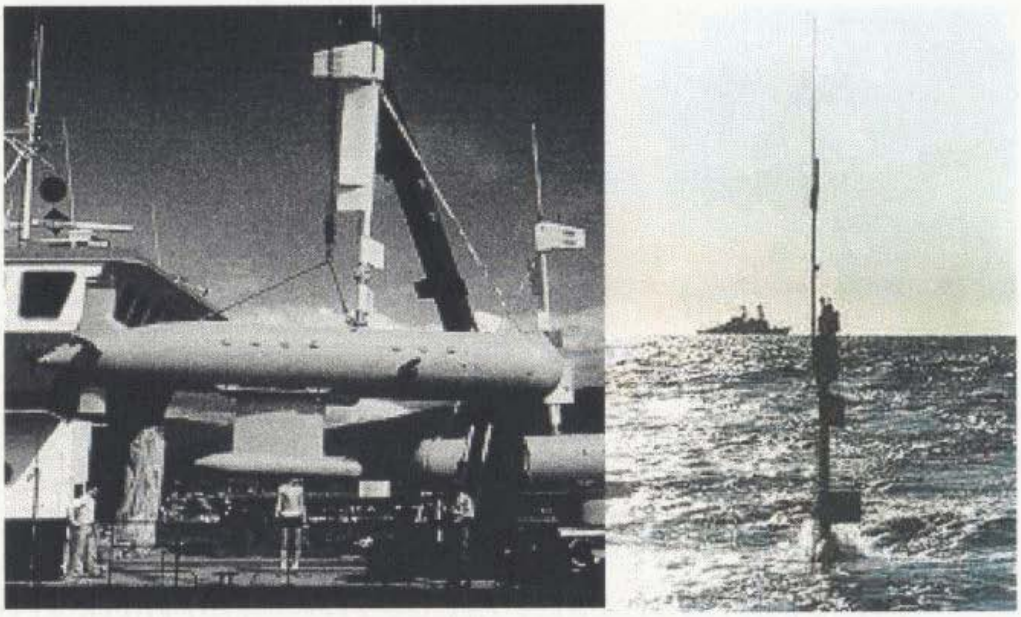

Figure 5.5.1: The surface AUV Dolphin being readied for operation (left, (Funnell, 1998)), and in a survey operation on the right (ISE, 2001). Note the snorkel for the Diesel engine intake and exhaust.

This type of surface-piercing vehicle is limited in its use, as it is affected by wave action, has limited stealth capabilities, and can see the ocean floor only in shallow waters. The advantage of this type of vehicle is that it can use an air-dependent propulsion system, since it needs a mast for the DGPS system anyway. The DOLPHIN uses a 212 hp, turbo-charged marine Diesel engine for main propulsion.

The most common, and most practical form of navigation and self-location is a differential GPS system to acquire a fix at the surface, plus an array of accelerometers, a true-north-seeking gyro compass, and a Doppler velocity log reflected off the seabed to

calculate a dead-reckoned position while the vehicle travels underwater (McFarlane, 1993). This method loses accuracy over time, but on short missions it has been shown to work well. For longer missions, vehicles generally surface at set time intervals to recalibrate their position for drift. Drift is comprised of two parts – electrical drift and physical drift. Electrical drift is the gradual change in the output of a circuit over time, and physical drift is the very slow movement of the vehicle due to outside forces over time such as ocean currents too slow for onboard accelerometers to measure. The drift associated with such a system is small enough that the AUV can navigate itself to where it needs to be, then use obstacle-avoidance sonar to fine-tune the docking or search procedure.

Navigation aboard C-SCOUT can be achieved through the use of an initial position fix, and then dead-reckoning using a combination of accelerometers and a three-axis gyro-compass. For tank testing, the initial fix can be determined by placing the vehicle in a known location in a known orientation. The location and orientation are relative to the test tank, and are arbitrary to the outside world. When put into ocean service, the initial fix can be found using a DGPS unit aboard the vehicle, and the AUV can surface periodically and check the actual position against the dead-reckoned position to correct for drift or errors in the navigational instruments. While underway, local navigation is enhanced through the use of an obstacle avoidance sonar placed in the nose module of the vehicle. C-SCOUT will also be outfitted with a magnetic compass which cannot be used

in the test tanks due to the metal rebar used in the reinforced concrete walls, but is intended to be used later in natural environments.

5.6 PROPOSED EMERGENCY SYSTEMS

The Failure Diagnostics and Error Recovery System is comprised of a power system monitor, an emergency ballast release, and flood sensors. The power system monitor watches the power usage and insures enough reserve energy is left to allow the vehicle to complete its mission or return home. It also checks for any short circuits or other conditions out of the ordinary, and acts as a surge suppressor for the entire system. This system has been installed on the C-SCOUT vehicle. The flood sensors are located at each end of the pressure vessel at the bottom. These can trigger the computer to abort the mission and return home as soon as possible. Chances are, however, that if the pressure vessel were going to leak, it would do so almost immediately upon placement in the water, since the o-rings make a very good seal once they seat themselves.

The emergency ballast release is the vehicle's last ditch effort to be recovered. A weight system, large enough to allow the vehicle to become fairly positively buoyant, is released near the nose. This forces the vehicle upwards to the surface for recovery. The weights are near the nose, so that if there is a malfunction and the propeller is still spinning, the vehicle will nevertheless rise and will not be forced back down by the propeller. It is important to note that this system would need to be modified if the vehicle were doing

interior pipeline inspections or under-ice operations. In those cases, it might be better for the vehicle to release a buoy with thin Kevlar® (Aramid) fibre line attached. This release system would allow the vehicle to sink to the bottom and the buoy to float to the surface under the ice where bore holes could be drilled, the buoy located with a pinger system, and the vehicle recovered. In a pipeline, the buoy would be dragged through the pipe by the fluid flow, and then a recovery could made by reeling in the line, or by sending another vehicle down the line. For ocean testing, a strobe beacon and pinger can be placed in the nose to facilitate recovery of the vehicle should such an emergency arise. However, the Baseline Configuration, does not require such an emergency system for use in the shallow, clear water test tanks within easy reach of divers.

Chapter 6 – Vehicle Deployment

6.1 C-SCOUT CARRIAGE

A carriage was made to hold C-SCOUT to make working on and transporting the vehicle within the building much easier. The carriage had three rails, each lined with inline-skate wheels, that allowed the AUV to be broken down into modules and split apart (Figure 6.1.1). The rails also make aligning the modules a quick and easy process for reassembling the vehicle. There is storage space below where the vehicle sits that is used to hold tools, flotation, and other peripherals.

Figure 6.1.1: C-SCOUT Carriage. Note the three rails of inline-skate wheels used to align and hold the modules during modification and re-assembly.

6.2 C-SCOUT LAUNCH PROCEDURE

The procedure for readying C-SCOUT for launch is as follows: During normal use, the only components removed from the vehicle during out of water time are the batteries, the pressure vessel, and any flotation foam obstructing them. The pressure vessel is sealed by bolting the lid on evenly, and then it can be slotted into the main module. There are dowels at each corner of the pressure vessel that slot into brackets mounted to the vehicle framework (Figure 6.2.1). These dowels make sure the circular pressure vessel is placed in the correct orientation and keep it from sliding back and forth.

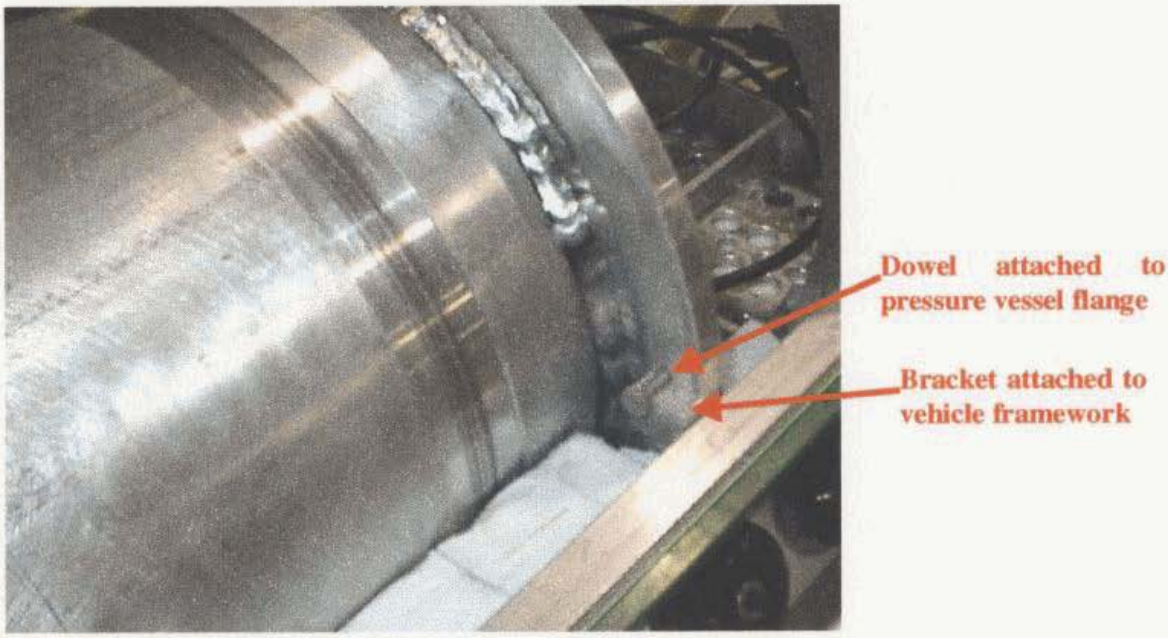

Figure 6.2.1: Pressure vessel dowel and mounting bracket

The next step is to connect the subsea connectors for the fin actuators, sonar, camera, main thruster, kill switches, and any other installed components. Then, the four large gray batteries can be placed in the battery trays with the leads directed away from the

centerline of the vehicle. The waterproof wiring that passes through the battery compartments should be placed in the tunnel between the two battery vent cover housings. The black computer batteries can then be placed on top to fully contain the wiring (See Figure 6.2.2). The waterproof connectors for the six batteries can then be plugged into the pressure vessel.

Figure 6.2.2: Battery stacking arrangement. Note cable tunnel between two lower batteries.

Flotation foam is then placed around the batteries and on top of the pressure vessel. An aluminum longitudinal stringer runs through the slots in the foam and bolts into the four module bulkheads. Adjustment screws on the stringer keep the pressure vessel snug in place and the batteries from sliding out of place (Figure 6.2.3).

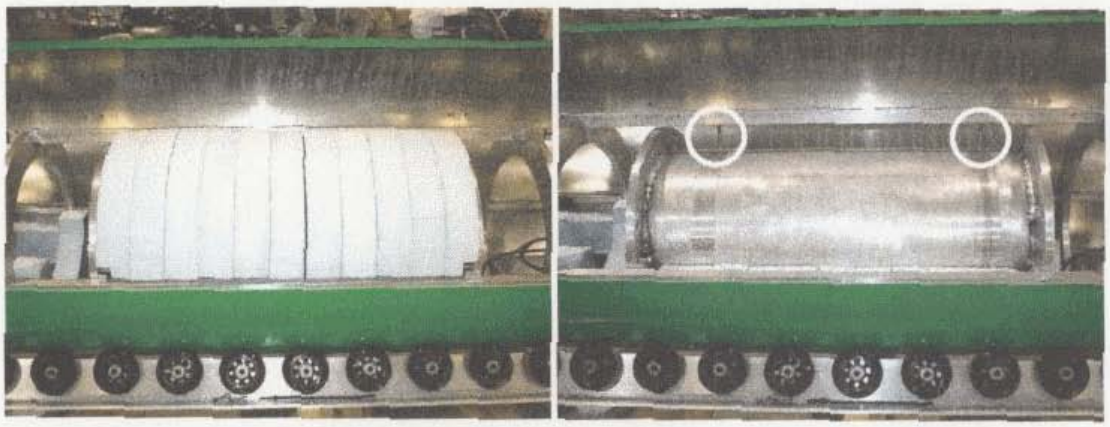

Figure 6.2.3: Stringer adjustment screws. Left picture shows foam and stringer in place, right picture shows foam removed *for clarity*.

Finally, the hinged skin can be closed and screwed in to the module bulkheads and longitudinal stringers. C-SCOUT is now ready to be powered up and deployed.

Chapter 7 – Vehicle Testing

7.1 C-SCOUT PRELIMINARY TESTING

The preliminary testing phase of the C-SCOUT AUV involved operating the vehicle using the Ethernet umbilical and was conducted in the Offshore Engineering Basin (OEB) (72 x 35 x 3.5 metres) at the Institute for Marine Dynamics. The main purpose of these tests was to demonstrate the vehicle operating in the water under operator control. The propulsor used for the tests was the trolling motor, which performed flawlessly. During the first test, the lower fin actuator failed so it lost encoder feedback to the computer system. This made the motor spin uncontrollably, eventually overheating the amplifier boards due to the high power consumed. The amplifier boards have automatic high-temperature cut-off switches, which disabled the actuator. Unfortunately, this overheating also disabled the thruster, and the vehicle had to be removed from the tank. Unplugging the disabled actuator from the pressure vessel and waiting a few minutes for the system to cool back down solved the problem and allowed testing to resume. The actuator motor had failed because it had flooded in a previous test and the encoder had corroded. The motor was replaced with a new one for future tests, and all of the actuators had an additional seal installed on the shaft to prevent further flooding.

The vehicle was controlled using a joystick connected to the laptop computer, which was set in the back of a small rowboat. The boat was paddled around beside the C-SCOUT to

prevent the umbilical from restricting the vehicle or snagging on a control surface or the propeller (Figure 7.1.1).

Figure 7.1.1: C-SCOUT being controlled through an Ethernet umbilical from a laptop and joystick inside the rowboat.

An emergency power-kill switch was also installed that provided an interrupt for the main AUV power systems should a problem arise due to loss of communication between the laptop computer and the onboard computer system. The anticipated mode of failure was either the laptop battery running out or the onboard computer batteries running out. The hardware used during the tests had no integral fail-safe built in, so if communications were lost with the host, the vehicle would maintain its last command. The hardwired emergency switch was tested by turning off power to the laptop computer while operating the vehicle, and then toggling the switch which stopped power to the vehicle systems instantly. This system was tested multiple times before launching and was used at the

very end of the test to prevent the propeller from accidentally spinning and injuring anyone during vehicle retrieval.

Another safety feature installed was a waterproof on/off switch for the onboard computer external to the pressure vessel. This switch was used to boot the computer system when the vehicle was ready to be placed in the water. Having an external-operated switch for the computer system conserved battery power while the vehicle was readied for launching and also enabled the system to be rebooted. Without an external on/off switch for the computer system, the computer would have to be booted up before the pressure vessel was bolted closed, placed in the vehicle, and the vehicle transported to the launch site and deployed. During this time, the computer system would be consuming valuable power and also heating up the other components inside the pressure vessel. Heat sinks were added to remove heat from the amplifiers and transfer it to the pressure vessel walls where it could be absorbed into the surrounding water. Communication between the laptop and the onboard computer could be established one minute and twenty seconds after the power had been turned on. It is crucial to have some form of external power switch for AUV testing to prevent damage to the vehicle or test facility from unforeseen failures.

The AUV was driven in left and right turning circles and in figure-eight maneuvers, and also dove up and down. In the main set of trials C-SCOUT dove to a depth of two metres limited only by the depth of the Offshore Engineering Basin. In a previous trial in the

Clear Water Towing Tank, C-SCOUT reached a depth of six metres. Vehicle motion response to control surface deflection was almost immediate – a noticeable yaw rate could be discerned within two to three seconds with the trolling motor operating at maximum power. The maximum speed achieved was approximately 0.5 metres per second from analyzing video footage. Turning circle diameters were approximately three body lengths (eight metres) with a control surface deflection of 25 degrees. Diving from the surface was a slow process as the nose of the vehicle had a tendency to trap a bubble of air. Using the control surfaces to bring the tail of the vehicle to the surface forced the nose down, allowing the AUV to dive. Once fully submerged, changing depth was straightforward.

The vehicle operated in the tank for nearly three hours and had no problems after the initial faulty motor. This successful trial provided a proof of concept test and mapped out the next set of vehicle modifications and testing (Figure 7.1.2).

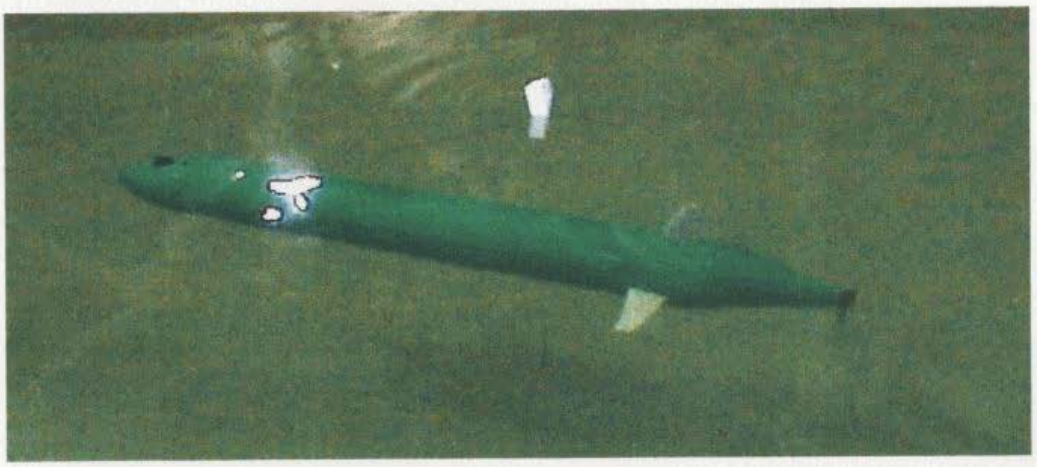

Figure 7.1.2: C-SCOUT operating entirely submerged.

Chapter 8 – Conclusions and Recommendations

8.1 CONCLUSIONS

This thesis has taken the C-SCOUT AUV from the concept stage to the drawing board to the test tanks. Although not yet autonomous, C-SCOUT has the capability to run untethered and is readily adaptable for autonomous operation.

The ease of construction and modification of the modular design has been proven. The second C-SCOUT vehicle was built by a student working alone in less than two months, including training in the machine shop. Having multiple nose and tail modules was especially beneficial as it allowed instrumentation and propulsion systems to be swapped in and out quickly and simply. The molds manufactured for the nose module, tail module, and control surfaces made the manufacturing of these complex shapes a simple job. The initial cost of the mold has been justified very quickly. Quick and easy access to the inside of the vehicle was also a benefit during testing so individual components could be monitored.

Detailed analysis of pressure vessel design resulted in an equation to assist engineers in determining which design is the most optimal from a weight standpoint. This equation

allows a user to input material properties and geometry of a cylindrical pressure vessel, and the minimum possible weight is returned.

External power switches for the computer power system and thruster/actuator power system aboard the vehicle were crucial to the debugging and testing phase. The two power systems could operate independently of one another and both could be instantly shut down in the event of an emergency situation. When the vehicle is fully autonomous, an acoustic transponder (hydrophone) should be included within the AUV and it should be provided with an independent power supply (battery) so that this safety feature can be activated at any time.

Having a dedicated vehicle carriage (trolley) also made working on the vehicle and transporting it a simple job. Large pneumatic tires should be installed on the next carriage so as to prevent jarring of the computer system while in transport.

The majority of required onboard equipment has been specified, and much of that has been purchased for future implementation. The preliminary tests to prove the modular vehicle design were successful and the AUV was found to be very easy to deploy, operate, and retrieve. The C-SCOUT is ready to serve as a testbed for graduate level research as planned.

8.2 RECOMMENDATIONS FOR FUTURE WORK

Throughout this thesis, many problems arose, and many areas of research surfaced that needed further examination. Several of these would make interesting and viable topics for future thesis work. Some of them are listed below:

- Develop a robust modular computer system for onboard control.
- Test vehicle hydrodynamics through turning circles, acceleration/deceleration, and figure-eight maneuvers.
- Develop an automatic trim and ballast system.
- Conduct endurance trials with the vehicle at a number of speeds.
- Install sonar, compass, GyroTrac system, and hydrophones and integrate them into system.
- Install emergency response system using hydrophones to communicate.
- Develop feedback system for AUV to communicate mission status to operators.
- Study and test control surfaces on submerged vehicles to derive equations of motion.
- Study alternate energy supplies or sources for underwater use.
- Study the possibility of creating an AUV from composites or roto-molding to lighten the weight and allow for more battery capacity.
- Study multiple-vehicle communication and behavior.

REFERENCES

1. Allmendinger, Eugene (1990). Submersible Vehicle Systems Design. Society of Naval Architects and Marine Engineers, New Jersey, USA.

2. Boileau, Renee (1999). Hull Structure Design for the Autonomous Underwater Vehicle C-SCOUT. Institute for Marine Dynamics. Report # LM-1999-03. Canada.

3. Funnell, Clifford (1998). Janes Underwater Technology. Edition 1, Jane's Information Group, Ltd. United Kingdom.

4. Granville, Paul S. (June 1976). Elements of the Drag of Underwater Bodies. David W. Taylor Naval Ship Research and Development Center, Report SPD-672-01, Bethesda, Maryland.

5. Healey, A. J., S.M. Rock, S. Cody, D. Miles, and J.P. Brown (1994). "Toward an Improved Understanding of Thruster Dynamics for Underwater Vehicles." Proceedings of the IEEE 1994 Symposium on Autonomous Underwater Vehicle Technology July 19-20, 1994 Cambridge, Massachusetts.

6. Healey, Anthony and Good, Michael (May 1992). The NPS AUV II Autonomous Underwater Vehicle Testbed: Design and Experimental Verification. Naval Engineers Journal, ASNE.

7. Hoerner, Sighard F. (1965). Fluid-Dynamic Drag. Published by the author. New Jersey, USA.

8. Humphreys, Douglas E. (1994). Improvement of the Low-Speed Control Authority of an AUV Through Hull Shaping. Vehicle Control Technologies, Inc. 11180 Sunrise Valley Drive – Suite 350, Reston, Virginia 20191 USA.

9. International Submarine Engineering, Ltd. (2001). *Autonomous Underwater Vehicles (AUV)*. http://www.ise.bc.ca.

10. Landsburg, Alexander and James Card (1983). Design and Verification for Adequate Ship Maneuverability. SNAME Transactions, Vol. 91, 1983.

11. Marine Systems Engineering Laboratory (2000). *Autonomous Undersea Systems Institute*. http://www.ausi.org.

12. McFarlane, James (1993). Development of Underwater Work Systems. International Submarine Engineering Ltd., Tutorial VII (F47), OCEANS '93, Victoria, British Columbia, Canada, IEEE.

13. Nahon, Meyer (1993). Determination of Undersea Vehicle Hydrodynamic Derivatives Using the USAF Datcom. Proceedings of OCEANS '93, Vol. II. Victoria, British Columbia, Canada, IEEE.

14. Paster, Donald L. (1986). Importance of Hydrodynamic Considerations for Underwater Vehicle Design. Raytheon Company – Submarine Signal Division. Rhode Island.

15. Potter, I.J., G.T. Reader, and J.G. Hawley (1992). Naval Architectural and Power System Selection for Underwater Vessels. Proceedings of the 1992 Symposium on Underwater Vehicle Technology, Washington DC.

16. Smith, S.M., K. Heeb, N. Frolund, and T. Pantelakis (1994). The Ocean Explorer AUV: A Modular Platform for Coastal Oceanography. Florida Atlantic University.

17. Smith, S.M., P.E. An, K. Ganesan, and S.E. Dunn (1995). Strategies for Simultaneous Multiple AUV Operation and Control. Ocean Engineering Department, Florida Atlantic University.

18. Tecnadyne Advanced Product Development (2001). *DC Brushless Thrusters*. www.tecnadyne.com/thrusters.htm.

19. URA Labs (1995).*Robot Design*. http://underwater.iis.u-tokyo.ac.jp/robot/r1/r1-chp2-e.html#propulsion.

20. Webb Research Corporation (2001). http://www.webbresearch.com.

BIBLIOGRAPHY

1. AAEON (1999). *PCM-7890 Pentium II Little Board with LCD, Ethernet, Audio, & 4 COMs*. www.aaeon.com/html/pcm7890.html.

2. Abbott, Ira and von Doenhoff, Albert (1959). Theory of Wing Sections. Dover Publications, Inc. New York.

3. Allen, Julian (1949). Estimation of the Forces and Moments Acting on Inclined Bodies of Revolution of High Fineness Ratio. National Advisory Committee for Aeronautics, Report RM A9I26, Washington D.C.

4. Animatics Corporation (2001). *Series 5000 Servo Control*. www.animatics.com/5000list.htm.

5. Benthos (2001). *Deep Sea Glass Spheres and Instrument Housings*. www.benthos.com/pdf/Spheres/instrument.pdf.

6. Corvallis Micro Technology, Inc. (1996). *CMT March Palm Sized GPS/GIS DataCollection*. www.cmtinc.com/fieldcmp/march.html.

7. Curtis, Timothy (1999). The Comprehensive Design of an Autonomous Underwater Vehicle. Senior Thesis, Webb Institute of Naval Architecture.

8. Curtis, Timothy (1999). Hull, powering and control surface design for the autonomous underwater vehicle C-SCoUT. Institute for Marine Dynamics, Report # LM-1999-01. Canada.

9. Deepsea Power & Light (2001). *Micro-SeaLite*. www.deepsea.com/microsl.html.

10. Electro Sales Co. Inc. (1996). *Hurst Motors: Geared Brushless DC Motor*. www.electrosales.com/hurst/4817-003.html.

11. Entran Sensors and Electronics (1998). *EGAS3 Miniature Rugged Triaxial Accelerometer*. www.entran.com/egas3.htm.

12. Flotation Technologies, FloTec (2000). *ROV and Submersible Flotation*. www.flotec.com/flo10.html.

13. Fossen, Thor I., and Fjellstad, Ola-Erik (1995). Nonlinear Modeling of Marine Vehicles in 6 Degrees of Freedom. Journal of Mathematical Modeling of Systems, Vol. 1, No. 1.

14. Ganer, Mesut and Glover, Edward (1994). Propeller/Stator Propulsors for Autonomous Underwater Vehicles. Proceedings of the IEEE 1994 Symposium on Autonomous Underwater Vehicle Technology July 19-20, 1994 Cambridge, Massachusetts.

15. Gertler, Morton (April 1950). Resistance Experiments on a Systematic Series of Streamlined Bodies of Revolution – For Application to the Design of High-Speed Submarines. David W. Taylor Model Basin, Report C-297, Washington D.C.

16. Gertler, Morton (July 1958). Application of the Lap-Troost Extrapolation Method to Submerged Bodies of Revolution. David Taylor Model Basin, Report 1236, Washington DC.

17. Gray, Lucas (1999). Construction of the C-SCOUT AUV. Institute for Marine Dynamics. Report # LM-1999-21. Canada.

18. Gray, Lucas (2000). C-SCOUT Progress : Summer 2000. Institute for Marine Dynamics. Report # LM-2000-14. Canada.

19. Holt, John K., and White, Dan G. (1994). High Efficiency, Counter-Rotating Ring Thruster for Underwater Vehicles. Harbor Branch Oceanographic Institution.

20. Hughes, Owen F. (1988). Ship Structural Design. Society of Naval Architects and Marine Engineers. New Jersey.

21. Humphreys, Douglas E. and Smith, Neill S. (1990) Hydrodynamics and Control of a Streamlined UUV Operating at 180-Degree Angle of Attack. California Research & Technology Division of TITAN Corp., 3033 Science Park Road San Diego, CA 92121 USA.

22. Lambert, J.D. (1960). The Effect of Changes in the Stability Derivatives on the Dynamic Behavior of a Torpedo. Admiralty Research Laboratory Report ARL/R3/HY/13/0, Ministry of Aviation, United Kingdom.

23. Landweber and Johnson (1951). Prediction of Dynamic Stability Derivatives of an Elongated Body of Revolution. David Taylor Model Basin Report C-359.

24. Lewis, Edward (1988). Principles of Naval Architecture, Volume II – Resistance, Propulsion and Vibration. Society of Naval Architects and Marine Engineers.

25. Munson, B., D.F. Young, and T.H. Okiishi (1994). Fundamentals of Fluid Mechanics. John Wiley and Sons, Inc. New York.

26. Nahon, Meyer (1996). A Simplified Model for Autonomous Underwater Vehicles. Proceedings of AUV '96. Monterey, CA, IEEE.

27. Radio-Tech Limited (1999). *Rtcom-Outback Modem.* www.radio-tech.co.uk/.

28. Read, Douglas (1997). A Computational Fluid Dynamic Investigation of Pressure Drag Reduction in Submarine Hull Forms. Senior Thesis, Webb Institute of Naval Architecture.

29. Reddy, D.V. and M. Arockiasamy (1991). Offshore Structures. Krieger Publishing Company. Florida.

30. Roark and Young (1982). Formulas for Stress and Strain. 5th Edition. (excerpt).

31. Rules for Certification/Classification of Submersibles. (1988). Det Norske Veritas. Norway.

32. Shigley, J. and Mischke, C. (1989). Mechanical Engineering Design, Fifth Edition. McGraw-Hill, Inc.

33. Smith, S.M., K. Ganesan, T. Flanigan, and L. Marquis (1995). The Intelligent Distributed Control System Architecture in the Ocean Voyager II and Ocean Explorer

Vehicles. Ocean Engineering Department, Florida Atlantic University, 777 Glades Rd., Boca Raton, FL 33431, USA.

34. Souders, William G. (1974). Turbulent Boundary Layer and Viscous Resistance of a Submarine at High Reynolds Number. Naval Ship Research and Development Center, Report 4366. Maryland.

35. Thomas, George B. and Ross L. Finney (1993). Calculus and Analytic Geometery. Addison-Wesley Publishing Company.

36. Tritech International Ltd. (1998). *SeaKing DFS Imaging Sonar*. www.tritech.co.uk.

37. Ultralife Batteries, Inc. (2001). *Solid Polymer Rechargeable Batteries*. http://www.ulbi.com/product-display.asp?ID=39 .

38. Whicker, L. Folger, and Leo Fehlner (1958). Free-Stream Characteristics of a Family of Low-Aspect-Ratio, All-Movable Control Surfaces for Application to Ship Design. David Taylor Model Basin, Report 933. Washington D.C.

39. Yardney Technical Products, Inc. (1999). *Silver Based Battery Systems*. www.yardney.com/yardney/silver.htm.

APPENDIX A
Powering Calculations

Surface area and volume calculations for the Baseline Configuration C-SCOUT

$\lambda := 6.75$	L/D Ratio (optimum = 7:1)	$Diam := 0.4 \cdot m$	Hull Diameter
	$Length := \lambda \cdot Diam$	$Length = 2.7 \cdot m$	Initial Hull Length
	$nose_L := .3\ m$	$tail_L := .5\ m$	
$PMB := \frac{(Length - nose_L - tail_L)}{Length} \cdot 100$		$PMB := 63.9\ \%$	Percent Parallel Mid-Body
$PMB_L := PMB \cdot Length$		$PMB_L = 1.725 \cdot m$	Length of Parallel Mid-Body

Surface Area:

$r := \frac{Diam}{2}$ Hull radius

$maj := nose_L$ Major nose ellipsoid axis

$maj = 0.3 \cdot m$

$min := r$ Minor nose ellipsoid axes

$min = 0.2 \cdot m$

note: ellipsoid nose is actually a prolate sphere (equations: CRC Standard Math Tables 29ed. p.112, 178)

eccentricity $e_{ellipse} := \frac{\sqrt{maj^2 - min^2}}{maj}$

$$SA_{prosphere} := 2 \cdot \pi \cdot \left(min^2 + \frac{maj \cdot min}{e_{ellipse}} \cdot asin\left(e_{ellipse}\right) \right)$$

$SA_{nose} := \frac{1}{2} \cdot SA_{prosphere}$ Nose module area

$SA_{nose} = 0.338 \cdot m^2$

$SA_{tail} := r \cdot \pi \cdot \sqrt{\left[\left(1 - \frac{1}{2 \cdot \lambda} - PMB \right) \cdot Length \right]^2 + r^2}$ Tail module area

$SA_{tail} = 0.503 \cdot m^2$

$SA_{midbody} := 2 \cdot \pi \cdot r \cdot PMB_L$ Area of parallel mid-body

$SA_{midbody} = 2.168 \cdot m^2$

$SA := SA_{nose} + SA_{midbody} + SA_{tail}$ Total surface area of hull

$SA = 3.009 \cdot m^2$

Volume:

$$V_{nose} := \frac{1}{2} \cdot \left(\frac{4}{3} \cdot \pi \cdot maj \cdot min \cdot min \right)$$

Volume of nose module

$$V_{nose} = 0.025 \cdot m^3$$

$$V_{newtail} := \frac{1}{3} \cdot \pi \left[r^2 + (.045 \cdot m)^2 + (r \cdot .045 \cdot m) \right] \cdot .5 \cdot m$$

Volume of tail module

$$V_{newtail} = 0.027 \cdot m^3$$

$$V_{PMB} := \pi \cdot r^2 \cdot PMB_L$$

Volume of parallel mid-body

$$V_{PMB} = 0.217 \cdot m^3$$

$$Volume := V_{nose} + \left(\pi \cdot r^2 \cdot Length \cdot PMB \right) + V_{newtail}$$

Total hull volume

$$Volume = 0.269 \cdot m^3$$

Drag from Granville slender bodies with parallel midbody at 4.12 m/s:

$\nu := 1.0537 \cdot 10^{-6} \cdot \frac{m^2}{sec}$ Kinematic Viscosity (SW, 20 C)

$\rho := 1025 \cdot \frac{kg}{m^3}$ Water Density (SW, 20 C)

$V := 4.12 \cdot \frac{m}{sec}$ Velocity

$D := 0.4 \cdot m$ Hull Diameter

$L := 6.75 \cdot D$ Hull Length

$L = 2.7 \cdot m$

$S := 3.009 \cdot m^2$ Surface Area

$Re := \frac{V \cdot L}{\nu}$ Reynolds Number

$Re = 1.056 \cdot 10^7$

$Cf := \left[\frac{.0776}{(\log(Re) - 1.88)^2}\right] + \frac{60}{Re}$ Flat plate drag coefficient

$Cf = 2.939 \cdot 10^{-3}$

$Cr_{low} := 0.1 \cdot 10^{-3}$ Form drag coefficient (estimated from chart ranging from smooth bodies to rough appendaged bodies, hence low and high)

$Cr_{high} := 1.1 \cdot 10^{-3}$

$Cd_{low} := Cf + Cr_{low}$ Drag Coefficent

$Cd_{high} := Cf + Cr_{high}$

$D_{low} := Cd_{low} \cdot \rho \cdot S \cdot V^2 \cdot \frac{1}{2}$ Actual Drag

$D_{low} = 8.111 \cdot kgf$ $D_{low} = 79.546 \cdot N$

$D_{high} := Cd_{high} \cdot \rho \cdot S \cdot V^2 \cdot \frac{1}{2}$

$D_{high} = 10.781 \cdot kgf$ $D_{high} = 105.723 \cdot N$

$Power_{low} := D_{low} \cdot V$ Power estimates

$Power_{high} := D_{high} \cdot V$

$Power_{low} = 327.731 \cdot watt$

$Power_{average} := \frac{(Power_{low} + Power_{high})}{2}$

$Power_{high} = 435.578 \cdot watt$

$Power_{average} = 381.654 \cdot watt$

Component Buildup Method from ARCS software:

$$Rt := 3 \cdot 10^5$$

$$Xt := v \cdot \frac{Rt}{V \cdot L}$$

$$C_{fT} := .455 \cdot (\log(Re))^{-2.58}$$

$$C_{ft} := .455 \cdot (\log(Rt))^{-2.58}$$

$$C_{fL} := 1.328 \cdot Rt^{-.5}$$

$$C_f := C_{fT} - Xt \cdot \left(C_{ft} - C_{fL}\right)$$

$$CDB := C_f \left[1 + 60 \cdot \left(\frac{D}{L}\right)^3 + .0025 \cdot \frac{L}{D}\right]$$

$$Te := \frac{CDB \cdot \left(\rho \cdot S \cdot V^2\right)}{2}$$

$Te = 9.336 \cdot kgf$

$$P := Te \cdot V$$

$P = 377.215 \cdot watt$

From Granville:

$Power_{average} = 381.654 \cdot watt$

From ARCS:

$P = 377.215 \cdot watt$

$$Error := \frac{\left|Power_{average} - P\right|}{Power_{average}}$$

Error:

$Error = 1.163 \cdot \%$

APPENDIX B

Control Surface Calculations

C-SCOUT Fin Sizing

Control Surface Sizing adapted from DnV rules: SNAME Vol 91, 1983

$d := 15.85 \cdot in$ Hull Diameter

$\lambda := 6.75$ L/B (Length/Beam) Ratio

$LBP := d \cdot \lambda$ Length Between Perpendiculars (Length Over-All)

$LBP = 106.987 \cdot in$

$T := d$ Draft

$B := d$ Beam

$$Area := \frac{T \cdot LBP}{100} \cdot \left[1 + 25 \cdot \left(\frac{B}{LBP} \right)^2 \right] \qquad Area = 26.262 \cdot in^2$$ Basic control surface size

For control surfaces not directly behind the propeller, DnV suggests an increase in rudder size by at least 30%.

$Area_{mod} := 1.30 \cdot Area$ $Area_{mod} = 34.141 \cdot in^2$ $Area_{mod} = 220.262 \cdot cm^2$

The NPS vehicle adds an additional factor of 50% to make the performance match that of empirical and tested data.

$Area_{adj} := 1.50 \cdot Area_{mod}$ $Area_{adj} = 51.211 \cdot in^2$ $Area_{adj} = 330.393 \cdot cm^2$

This area will be for each control surface (one face). Since this vessel is rotationally symmetrical, the dive planes will be the same size as the rudders. The actual dimensions are calculated as follows:

original Aspect Ratio (length/tip width) $oldAR := \frac{18}{6}$ $oldAR = 3$

original Taper Ratio (base width/tip width) $oldTR := \frac{15}{6}$ $oldTR = 2.5$

keeping Taper Ratio approx. the same:

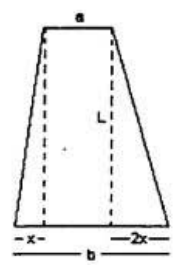

$b := 6.1 \, in$ Width of fin base

$x := 3.1 \cdot cm$ Taper of leading edge

$a := b - 3 \, x$ $a = 6.194 \cdot cm$ Width of fin tip

$L := 5.33 \, a$ $L = 33.014 \cdot cm$ Length of fin

$TR := \frac{b}{a}$ $TR = 2.501$ Taper Ratio

$AR := \frac{L}{a}$ $AR = 5.33$

$$A := L \cdot \left(a + \frac{3}{2} \cdot x \right) \qquad A = 358.004 \cdot cm^2$$ Area of one side of fin

Comparing this fin with the required area:

$A = 358.004\ cm^2$ $\quad Area_{adj} = 330.393\ cm^2$

$A = 55.491\ in^2$ $\quad Area_{adj} = 51.211\ in^2$

$\frac{A - Area_{adj}}{Area_{adj}} = 8.357\%$ Percent difference between required control surface area and required fin

$J := \frac{2 \cdot A}{Area_{mod}}$ $\quad J = 3.251$ This is the ratio of scaling from DnV rules, and can be compared to NPS AUV II in the Excel worksheet fins.xls

$D_{Turning\_Circle} := .3122 \cdot J^2 - 2.7385 \cdot J + 8.401$ from Excel

$D_{Turning\_Circle} = 2.798$ in vehicle lengths

Location of control rod (shaft):

$Top := \frac{a}{4} + x$

$Bottom := \frac{(3 \cdot x + a)}{4}$

$Shaft := \frac{Top - Bottom}{3} + Bottom$

$Shaft = 1.627\ in$ from front edge of control surface

$t := 0.15$ NACA Section Number of Symmetrical Foil

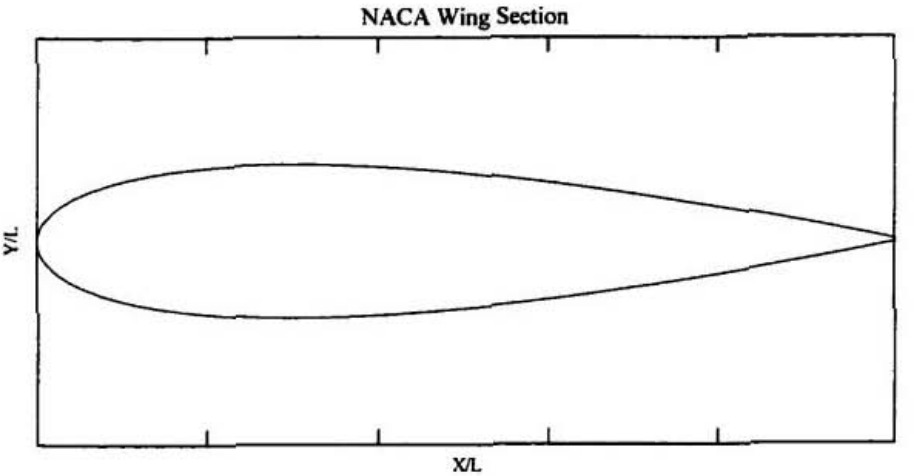

APPENDIX C

Pressure Vessel Design

In an attempt to totally optimize the pressure vessel weight for the desired depth, I shall bring all of the failure modes together so that they should theoretically occur at the same depth. By doing this, no single failure mode will be overbuilt, and therefore the pressure vessel will have the least amount of mass.

$\sigma_{YS} := 296\ MPa$ $\quad$ $v := 0.334$

$E := 71\ GPa$ $\quad$ $\rho_{al} := 2770 \frac{kg}{m^3}$

$L := 22\ in$ Length of Pressure Vessel

$R := \frac{15.177\ in}{3}$ Internal Radius $\quad R = 5.059 \cdot in$

$N := 6$ Number of Stiffeners

$L_f := \frac{L}{N}$ Length between frames

$A_f := 1.2\ in^2$ Cross sectional area of stiffener

$n := 5000$

Program1 :=

$x \leftarrow 0$

for $J \in 1, 2 .. n$

$t \leftarrow x \cdot in$

$PY \leftarrow \frac{\sigma_{YS}}{R} \cdot \left(t + \frac{A_f}{L_f} \right)$

$PM \leftarrow \frac{2.42 \cdot E \cdot \left(\frac{t}{2 \cdot R} \right)^{\frac{5}{2}}}{\left(1 - v^2 \right)^{\frac{3}{4}} \cdot \left[\frac{L_f}{2 \cdot R} - 0.45 \cdot \left(\frac{t}{2 \cdot R} \right)^{\frac{1}{2}} \right]}$

$x \leftarrow x + \frac{.00001}{psi} \cdot (PY - PM)$ if $PY \neq PM$

break otherwise

x

Program1 = 0.190267890325

Thickness of shell - chosen to set the yield pressure and buckling pressure equal, since t is the only true variable in them.

$t := Program1 \cdot in$

$\lambda := \pi \cdot \frac{R}{L}$ $\lambda = 0.722$

$n := 2$ Number of circumferential lobes - iterated as 1,2,3... until pressure is a minimum.

$R_f := R + \frac{t}{2}$ Mean shell radius

$n1 := 5000$

Program2 :=
$x \leftarrow 0$
for $J \in 1, 2 .. n1$
$I \leftarrow x \cdot in^4$
$PY \leftarrow \frac{\sigma_{YS}}{R} \cdot \left(t + \frac{A_f}{L_f}\right)$
$PCR \leftarrow \frac{E \cdot t}{R} \cdot \left[\frac{\lambda^4}{\left(n^2 - 1 + \frac{\lambda^2}{2}\right) \cdot \left(n^2 + \lambda^2\right)^2}\right] + \frac{\left(n^2 - 1\right) \cdot E \cdot I}{R_f^3 \cdot L_f}$
$x \leftarrow x + \frac{0.000001}{psi} (PY - PCR)$ if $PY \neq PCR$
break otherwise
x

Program2 = 0.045662501

Required moment of inertia

$I_{req} := Program2 \cdot in^4$

$$P_Y := \frac{\sigma_{YS}}{R} \cdot \left(t + \frac{A_f}{L_f} \right)$$ Local yield pressure

$P_Y = 4392 \cdot psi$

$$P_M := \frac{2.42 \cdot E \cdot \left(\frac{t}{2 \cdot R} \right)^{\frac{5}{2}}}{\left(1 - \nu^2 \right)^{\frac{3}{4}} \cdot \left[\frac{L_f}{2 \cdot R} - 0.45 \cdot \left(\frac{t}{2 \cdot R} \right)^{\frac{1}{2}} \right]}$$ Buckling Pressure

$P_M = 4392 \cdot psi$

To calculate the moment of inertia:

$nl := 500000$

$a_{req} :=$ | $a \leftarrow 0.001\ in$
for $J \in 1, 2 .. nl$
$b \leftarrow \frac{A_f}{a}$
$CG \leftarrow \frac{\left(L_f t \cdot \frac{t}{2} \right) + a \cdot b \cdot \left(\frac{a}{2} + t \right)}{L_f t + a \cdot b}$
$I_{skin} \leftarrow \frac{L_f t^3}{12}$
$I_{flange} \leftarrow \frac{b \cdot a^3}{12}$
$I_l \leftarrow \left[I_{skin} + L_f t \cdot \left(CG - \frac{t}{2} \right)^2 \right] + \left[I_{flange} + a \cdot b \cdot \left[CG - \left(\frac{a}{2} + t \right) \right]^2 \right]$
$a \leftarrow a + \frac{0.1}{in^3} \cdot \left(I_{req} - I_l \right)$ if $I_l \neq I_{req}$
break otherwise
| a

$a_{req} = 0.345296535 \cdot in$

$I := I_{req}$

$a := a_{req}$

$n = 2$

$b := \frac{A_f}{a_{req}}$

$n := 2$

$b = 3.475 \cdot in$

$L_f - b = 0.191 \cdot in$

$$P_{CR} := \frac{E \cdot t}{R} \cdot \left[\frac{\lambda^4}{\left(n^2 - 1 + \frac{\lambda^2}{2}\right) \cdot \left(n^2 + \lambda^2\right)^2} \right] + \frac{\left(n^2 - 1\right) \cdot E \cdot I}{R_f^3 \cdot L_f}$$

Critical Pressure

$P_{CR} = 4392 \cdot psi$

$P_Y \cdot 33 \frac{ft}{atm} = 9862 \cdot ft$

$P_M \cdot 33 \frac{ft}{atm} = 9862 \cdot ft$

$P_{CR} \cdot 33 \frac{ft}{atm} = 9862 \cdot ft$

These depths are all the same, and this is the failure depth for the pressure vessel, therefore this is optimized with respect to weight for this depth.

The weight of this pressure vessel with the ring stiffeners can then be determined to be:

$$V_{ring} := \pi \left[(R + t + a)^2 - (R + t)^2 \right] \cdot b$$

$V_{ring} = 40.88 \cdot in^3$

$$V_{cyl} := \pi \cdot \left[(R + t)^2 - R^2 \right] \cdot L$$

$V_{cyl} = 135.558 \cdot in^3$

$$M_{total} := \rho_{al} \cdot \left(V_{cyl} + N \cdot V_{ring} \right)$$

$M_{total} = 38.112 \cdot lb$

APPENDIX D

Testing Phase Two

D.1 MODIFICATIONS FOR FUTURE TESTING

After the preliminary testing, several design modifications were suggested to a series of tests to determine the hydrodynamic characteristics of the C-SCOUT AUV, including turning circles, figure-eights, and stopping/starting performance. These modifications included the replacement of the Ethernet umbilical with a wireless Ethernet adapter, the use of a precision tracking system to determine vehicle performance, the complete implementation of the Tecnadyne thruster, and increased reliability in the computer system.

D.2 WIRELESS ETHERNET ADAPTER

The radio transmitter was installed to eliminate the effects of the umbilical dragging on the vehicle, but in itself required another restriction – a mast. Radio waves, like GPS signals, are quickly attenuated in water and therefore some way to bring the vehicle antenna to the surface is required. Attaching a small, streamlined mast to the vehicle at the predicted yaw center (Figure D.2.1) had a relatively small effect on vehicle performance, but confined the vehicle to a two-dimensional realm near the surface. This limitation is acceptable for the next set of trials described in a thesis by graduate student Roy Thomas. The addition of the mast also allowed operation of the AUV from a distance without having to follow the vehicle around the tank in a boat.

Figure D.2.1: The streamlined mast attached to the AUV C-SCOUT with tracking spheres and wireless Ethernet adapter mounted.

D.3 C-SCOUT MOTION CAPTURE DURING TESTING

Since the C-SCOUT AUV is not yet fully instrumented with sensors to measure position and orientation, an external system is required for the preliminary testing phase. The original plan was to use a QUALYSIS tracking system which consisted of six ultraviolet strobing spheres attached to the model that were tracked by cameras mounted around the tank perimeter. This system would have to be attached to the vehicle above the waterline on the mast. Each strobing sphere, including the individual electronics package, battery, and wiring, weighed 160 grams. Six of these plus a mounting tree for them would add a considerable weight to the top of the mast which may have caused stability problems for

the vehicle due to the tiny waterplane area of the mast. In addition, mounting expensive electronics on a marginally stable vehicle close to the water caused some concern.

A recently acquired vision-based tracking system was acquired by IMD in the first quarter of 2001. This system, the Peak Performance MOTUS, uses software to track high-contrast markers filmed by any video camera. The tracking is carried out in post-processing using the actual images, so if a marker were to become lost or overlapped, the software can be shown where the marker really is by manually clicking on it with the mouse. With the QUALYSIS system, if two markers temporarily overlap and the cameras confuse them, the whole data set can be invalidated.

The MOTUS System can work underwater, or through the water, so the original plan was to place reflective stickers on the hull of C-SCOUT and track them in two-dimensions using an overhead camera mounted in the ceiling of the tank. Test samples of this tracked very well, although any interference caused by waves or ripples would distort the underwater image giving false data. Also, as C-SCOUT moved farther from underneath the camera, the parallax error increased due to the angle of incidence of the light on the water's surface. Since a mast was used for the wireless Ethernet adapter, it made sense to attach a lightweight tracking tree to it. This tracking tree was constructed from tapered carbon-fibre tubes with Styrofoam® spheres impaled on the ends (See Figure D.3.1). These spheres were covered in reflective tape with a circle of black construction paper tacked below them like a saucer. The circle of black paper ensured high contrast between

the marker and whatever was below it, whether that be the vehicle, the water surface, an object on the bottom of the tank, or a reflection of an overhead light on the water.

Figure D.3.1: Styrofoam tracking spheres mounted on carbon-fibre rods with black construction paper saucers for consistent image tracking.

To accommodate a wider field of view for maneuvers, a wide angle lens can be mounted to the camera. This lens gave a workable water area of approximately 10 metres x 8 metres with minimal distortion. The MOTUS System tracks an object of similar color, locates its center of geometry, and tracks this point as the object. The highest accuracy possible is achieved by using a very consistent shape at all angles, a sphere, which was made as small as possible but still clearly visible by the camera. The resolution of the camera can be used to determine the workable area of the tank. The size of one pixel at the water surface can be calculated, and this value is the minimum size of a marker on the water surface that the setup system could detect.

D.4 SUGGESTED PHASE TWO OF PRELIMINARY VEHICLE TESTING

The first testing phase of the AUV provided proof-of-concept testing for the C-SCOUT AUV. The recommended second phase is to measure the performance of the vehicle with respect to the initial design specifications.

These preliminary tests will include starting and stopping performance, forward and reverse acceleration performance, and turning circles. The starting performance tests are carried out by bringing the vehicle from rest to a particular velocity in both forward and reverse, and measuring the time and distance covered. The stopping performance tests consist of the vehicle traveling at a set velocity, again both forward and reverse, and stopping the main propulsor. Additional stopping tests will be carried out using full negative thrust from the propulsor to simulate a crash stop. The time and distance covered until the velocity reached zero should be measured. The acceleration tests in forward and reverse consist of starting the vehicle from rest and applying full thrust and measuring the acceleration until top speed is reached. The turning circle tests consist of running the AUV at a constant speed and fin angle, and then measuring the diameter of the turning circle and the time taken for one complete revolution. The fin angle is then changed and the test run again. This systematic test should be completed for a number of speeds and fin angles. Figure D.4.1 shows the proposed test matrix.

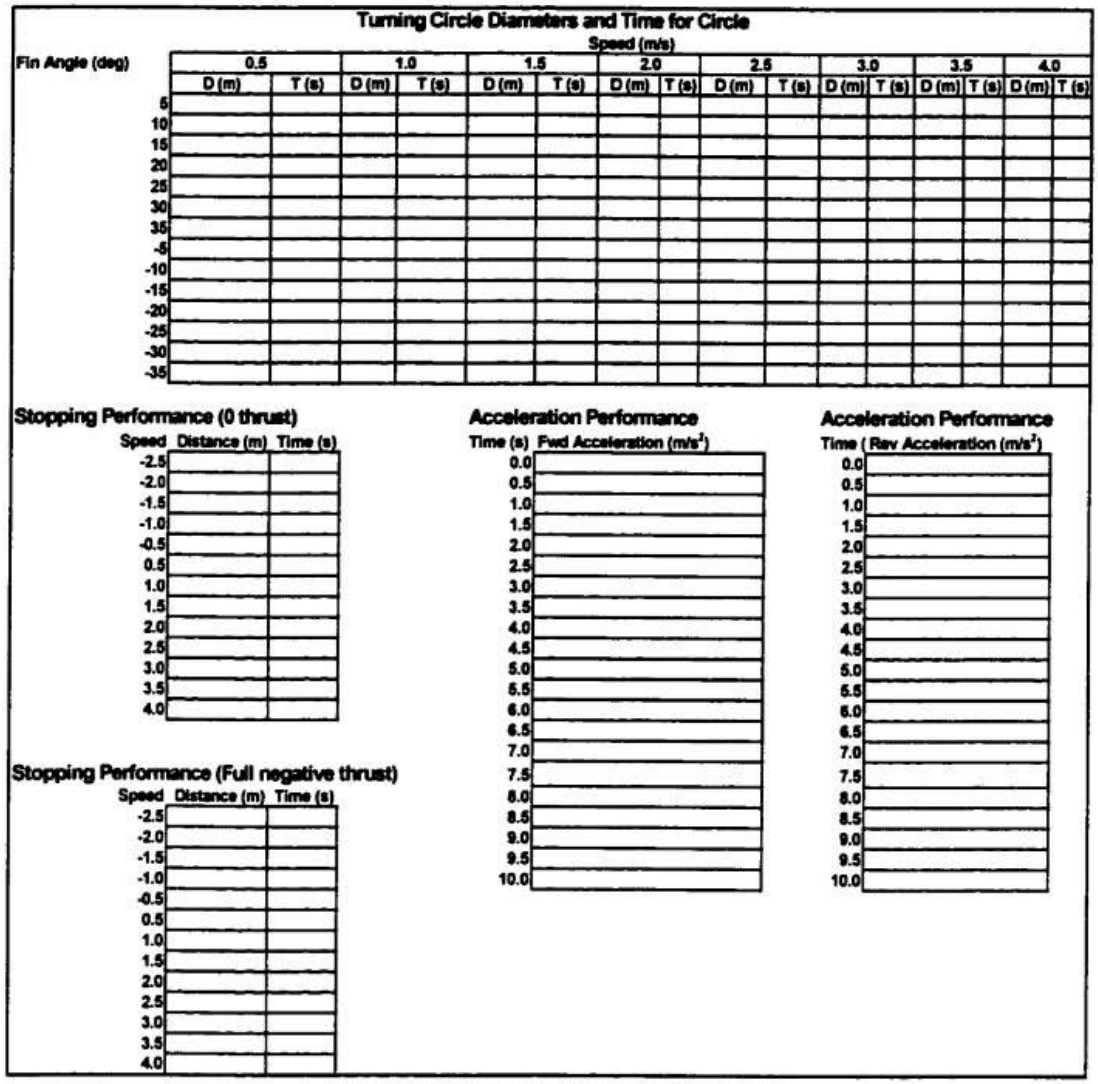

Figure D.4.1: Proposed phase-two test matrix.